

# Pseudo-Marginal Hamiltonian Monte Carlo

Fredrik Lindsten\* and Arnaud Doucet†

April 7, 2022

## Abstract

Bayesian inference in the presence of an intractable likelihood function is computationally challenging. When following a Markov chain Monte Carlo (MCMC) approach to approximate the posterior distribution in this context, one typically either uses MCMC schemes which target the joint posterior of the parameters and some auxiliary latent variables or pseudo-marginal Metropolis–Hastings (MH) schemes which mimic a MH algorithm targeting the marginal posterior of the parameters by approximating unbiasedly the intractable likelihood. In scenarios where the parameters and auxiliary variables are strongly correlated under the posterior and/or this posterior is multimodal, Gibbs sampling or Hamiltonian Monte Carlo (HMC) will perform poorly and the pseudo-marginal MH algorithm, as any other MH scheme, will be inefficient for high dimensional parameters. We propose here an original MCMC algorithm, termed pseudo-marginal HMC, which approximates the HMC algorithm targeting the marginal posterior of the parameters. We demonstrate through experiments that pseudo-marginal HMC can outperform significantly both standard HMC and pseudo-marginal MH schemes.

## 1 Introduction

Let  $y \in \mathcal{Y}$  be the observations and  $\theta \in \Theta \subseteq \mathbb{R}^d$  denotes the parameters of interest. We denote by  $\theta \mapsto p(y | \theta)$  the likelihood of the observations and we assign a prior for  $\theta$  of density  $p(\theta)$  with respect to Lebesgue measure  $d\theta$ . Hence the posterior density of interest is given by

$$\pi(\theta) = p(\theta | y) \propto p(y | \theta)p(\theta). \quad (1)$$

For complex Bayesian models, the posterior (1) needs to be approximated numerically. When the likelihood  $p(y | \theta)$  can be evaluated pointwise, this can be achieved using standard MCMC schemes. However, we will consider here the scenario where  $p(y | \theta)$  is intractable, in the sense that it cannot be evaluated pointwise. We detail below two important scenarios where an intractable likelihood occurs.

**Example: Latent variable models.** Consider observations  $y = y_{1:T}$  such that

$$X_k \stackrel{\text{i.i.d.}}{\sim} f_\theta(\cdot), \quad Y_k | X_k \sim g_\theta(\cdot | X_k), \quad (2)$$

where  $(X_k)_{k \geq 1}$  are  $\mathbb{R}^n$ -valued latent variables,  $(Y_k)_{k \geq 1}$  are  $\mathbb{Y}$ -valued (thus,  $\mathcal{Y} = \mathbb{Y}^T$ ) and  $i : j := \{i, i+1, \dots, j\}$  for any  $i < j$ . Having observed  $Y_{1:T} = y_{1:T}$ , the likelihood is given by  $p(y_{1:T} | \theta) = \prod_{k=1}^T p(y_k | \theta)$ , where each term  $p(y_k | \theta)$  satisfies

$$p(y_k | \theta) = \int_{\mathbb{R}^n} f_\theta(x_k) g_\theta(y_k | x_k) dx_k. \quad (3)$$

---

\*Department of Information Technology, Uppsala University, Sweden.

†Department of Statistics, Oxford University, UK.

If the integral (3) cannot be computed in closed form then the likelihood  $p(y_{1:T} | \theta)$  is intractable.

**Example: Approximate Bayesian computation (ABC).** Consider the scenario where  $\theta \mapsto \tilde{p}(y | \theta)$  is the “true” likelihood function. We cannot compute it pointwise but we assume we are able to simulate some pseudo-observations  $Z \sim \tilde{p}(\cdot | \theta)$  using  $Z = \gamma(\theta, V)$  where  $V \sim \lambda(\cdot)$  for some auxiliary variable distribution  $\lambda$  and mapping  $\gamma : \Theta \times \mathcal{V} \rightarrow \mathcal{Y}$ . Given a kernel  $K : \mathcal{Y} \times \mathcal{Y} \rightarrow \mathbb{R}^+$ , the ABC approximation of the posterior is given by (1) where the intractable ABC likelihood is

$$p(y | \theta) = \int_{\mathcal{Y}} K(y|z) \tilde{p}(z | \theta) dz = \int K(y|\gamma(\theta, v)) \lambda(v) dv. \quad (4)$$

Two standard approaches to perform MCMC in these scenarios are:

1. Implement standard MCMC algorithms to sample from the joint distribution of the parameters and auxiliary variables; e.g. in the latent variable context we would target  $p(\theta, x_{1:T} | y_{1:T}) \propto p(\theta) \prod_{k=1}^T f_\theta(x_k) g_\theta(y_k | x_k)$  and in the ABC context  $p(\theta, v | y) \propto p(\theta) \lambda(v) K(y | \gamma(\theta, v))$ . Gibbs type approaches sampling alternately the parameters and the auxiliary variables can converge very slowly if these variables are strongly correlated under the target [1, Section 2.3]. Hamiltonian Monte Carlo (HMC) methods allow to update efficiently both set of variables jointly [10]. However, they are typically unable to explore multimodal targets [19, Section 5.5.7].
2. Use a pseudo-marginal MH algorithm which replace the intractable likelihood term by a non-negative unbiased estimate of the true likelihood; see [1, 2, 4, 11, 16]. For example, in the ABC context the pseudo-marginal MH algorithm is a MH algorithm targeting  $p(\theta, v | y)$  using a proposal distribution  $q(\theta, \theta') \lambda(v')$ . As for any MH algorithm, it can be difficult to select the proposal  $q(\theta, \theta')$  when  $\Theta$  is high-dimensional.

In many scenarios, the marginal posterior (1) will have a “nicer” structure than the joint posterior of the parameters and auxiliary variables which often exhibit complex patterns of dependence and multimodality. For example, discrete choice models are a widely popular class of models in health economics, e-commerce, marketing and social sciences used to analyze choices made by consumers/individuals/businesses [22]. When the population is heterogeneous, such models can be represented as (2) where  $f_\theta(\cdot)$  is a mixture distribution, the number of components representing the number of latent classes; see e.g. [6]. In this context, the paucity of data typically available for each individual is such that the joint posterior  $p(\theta, x_{1:T} | y_{1:T}) = p(\theta | y_{1:T}) \prod_{k=1}^T p(x_k | y_k, \theta)$  will be highly multimodal while the marginal  $p(\theta | y_{1:T})$  will only have symmetric well-separated modes for  $T$  large enough, or one mode if constraints on the mixture parameters are introduced. Such problems also arise in biostatistics [13]. In these scenarios, current MCMC methods will be inefficient. In this article, we propose a novel HMC scheme, termed pseudo-marginal HMC, which mimicks the HMC algorithm targeting the posterior (1) while integrating out numerically the auxiliary variables. The method is a so called *exact approximation* in the sense that its limiting distribution (marginally in  $\theta$ ) is precisely  $\pi(\theta)$ . Previous approaches to this problem either do not preserve the invariant distribution of interest [17] or relies on an approximation of the gradient obtained by fitting an exponential family model in a Reproducing Kernel Hilbert space [21] which requires selecting an appropriate kernel.

## 2 Hamiltonian dynamics

### 2.1 Standard Hamiltonian dynamics

The Hamiltonian formulation of classical mechanics is at the core of HMC methods. Recall that  $\theta \in \Theta \subseteq \mathbb{R}^d$ . We identify the potential energy as the negative unnormalized log-target and introduce a momentum variable  $\rho \in \mathbb{R}^d$  which defines the kinetic energy  $\frac{1}{2}\rho^T\rho$  of the system<sup>1</sup>. The resulting Hamiltonian is given by

$$H_{\text{ex}}(\theta, \rho) = -\log p(\theta) - \log p(y | \theta) + \frac{1}{2}\rho^T\rho. \quad (5)$$

We associate a probability density on  $\mathbb{R}^d \times \mathbb{R}^d$  to this Hamiltonian through

$$\pi(\theta, \rho) \propto \exp(-H_{\text{ex}}(\theta, \rho)) = \pi(\theta)\mathcal{N}(\rho | 0_d, I_d), \quad (6)$$

where  $\mathcal{N}(z | \mu, \Sigma)$  denotes the normal density of argument  $z$ , mean  $\mu$  and covariance  $\Sigma$ .

Assuming that the prior density and likelihood function are continuously differentiable, the Hamiltonian dynamics correspond to the equations of motion

$$\frac{d\theta}{dt} = \nabla_\rho H_{\text{ex}} = \rho, \quad \frac{d\rho}{dt} = -\nabla_\theta H_{\text{ex}} = \nabla_\theta \log p(\theta) + \nabla_\theta \log p(y | \theta). \quad (7)$$

We will write

$$\varphi(\theta, \rho) = \begin{pmatrix} \rho \\ \nabla_\theta \log p(\theta) + \nabla_\theta \log p(y | \theta) \end{pmatrix}. \quad (8)$$

A key property of this dynamics is that it preserves the Hamiltonian, i.e.  $H_{\text{ex}}(\theta(t), \rho(t)) = H_{\text{ex}}(\theta(0), \rho(0)) = H_0$  for any  $t \geq 0$ . This enables large moves in the parameter space to be made by simulating the Hamiltonian dynamics. However, to sample from the posterior, it is necessary to explore other level sets of the Hamiltonian; this can be achieved by periodically updating the momentum  $\rho$  according to its marginal under  $\pi$ , i.e.  $\rho \sim \mathcal{N}(0_d, I_d)$ .

The Hamiltonian dynamics only admit a closed-form solution in very simple scenarios, e.g. if  $\pi(\theta)$  is normal. Hence, in practice, one usually needs to resort to a numerical integrator—typically, the Verlet method, also known as the Leapfrog method, is used due to its favourable properties in the context of HMC [14, p. 60], [19, Section 5.2.3.3]. In particular, this integrator is symplectic which implies that the Jacobian of the transformation  $(\theta(0), \rho(0)) \rightarrow (\theta(t), \rho(t))$  is unity for any  $t > 0$ . Because of numerical integration errors, the Hamiltonian is not preserved along the discretized trajectory but this can be accounted for by an MH rejection step. The resulting HMC method is given by the following: at state  $\theta := \theta(0)$ , (i) sample the momentum variable  $\rho(0) \sim \mathcal{N}(0_d, I_d)$ , (ii) simulate approximately the Hamiltonian dynamics over  $L$  discrete time steps using a symplectic integrator, yielding  $(\theta(L), \rho(L))$ , and (iii) accept  $(\theta(L), \rho(L))$  with probability  $1 \wedge \pi(\theta(L), \rho(L))/\pi(\theta(0), \rho(0)) = 1 \wedge \exp(H_{\text{ex}}(\theta(0), \rho(0)) - H_{\text{ex}}(\theta(L), \rho(L)))$ . We refer to [19] for details and a more comprehensive introduction.

### 2.2 Pseudo-marginal Hamiltonian dynamics

When the likelihood is intractable, it is not possible to use standard symplectic integrators to approximate numerically the Hamiltonian dynamics (7) as these integrators require being able to evaluate  $\nabla_\theta \log p(y | \theta)$  pointwise. We will address this difficult by instead considering a Hamiltonian system defined on an extended phase space when the following Assumptions hold.

---

<sup>1</sup>For simplicity we assume unit mass. The extension to a general mass matrix is straightforward.

- **Assumption 1.** There exists  $(\theta, \mathbf{u}) \mapsto \hat{p}(y | \theta, \mathbf{u}) \in \mathbb{R}^+$  where  $\mathbf{u} \in \mathcal{U}$  and  $m(\cdot)$  a probability density on  $\mathcal{U}$  such that  $p(y | \theta) = \int \hat{p}(y | \theta, \mathbf{u})m(\mathbf{u})d\mathbf{u}$ .

Assumption 1 equivalently states that  $\hat{p}(y | \theta, \mathbf{U})$  is a non-negative unbiased estimate of  $p(y | \theta)$  when  $\mathbf{U} \sim m(\cdot)$ . This assumption is at the core of pseudo-marginal methods [2, 8, 16, 18] which rely on the introduction of an extended target density

$$\bar{\pi}(\theta, \mathbf{u}) = \pi(\theta) \frac{\hat{p}(y | \theta, \mathbf{u})}{p(y | \theta)} m(\mathbf{u}) \propto p(\theta) \hat{p}(y | \theta, \mathbf{u}) m(\mathbf{u}). \quad (9)$$

This extended target admits  $\pi(\theta)$  as a marginal under Assumption 1. The pseudo-marginal MH algorithm is for example a ‘standard’ MH algorithm targeting (9) using the proposal  $q(\theta, \theta')m(\mathbf{u}')$  when in state  $(\theta, \mathbf{u})$ , resulting in an acceptance probability

$$1 \wedge \frac{p(\theta') \hat{p}(y | \theta', \mathbf{u}')}{p(\theta) \hat{p}(y | \theta, \mathbf{u})} \frac{q(\theta', \theta)}{q(\theta, \theta')}. \quad (10)$$

Instead of exploring the extended target distribution  $\bar{\pi}(\theta, \mathbf{u})$  using an MH strategy, we will rely here on an HMC mechanism. Our method will use an additional assumption on the distribution of the auxiliary variables and regularity conditions on the simulated likelihood function  $\hat{p}(y | \theta, \mathbf{u})$ .

- **Assumption 2.**  $\mathcal{U} = \mathbb{R}^D$ ,  $m(\mathbf{u}) = \mathcal{N}(\mathbf{u} | 0_D, I_D)$  and  $(\theta, \mathbf{u}) \mapsto \hat{p}(y | \theta, \mathbf{u})$  is continuously differentiable and  $(\theta, \mathbf{u}) \mapsto \log \nabla \hat{p}(y | \theta, \mathbf{u})$  can be evaluated pointwise.

Our algorithm will leverage the fact that  $m(\mathbf{u})$  is a normal distribution. Assumptions 1 and 2 will be standing assumptions from now on and allow us to define the following extended Hamiltonian

$$H(\theta, \rho, \mathbf{u}, \mathbf{p}) = -\log p(\theta) - \log \hat{p}(y | \theta, \mathbf{u}) + \frac{1}{2} \left\{ \rho^T \rho + \mathbf{u}^T \mathbf{u} + \mathbf{p}^T \mathbf{p} \right\}, \quad (11)$$

with a corresponding joint probability density on  $\mathbb{R}^{2d+2D}$

$$\bar{\pi}(\theta, \rho, \mathbf{u}, \mathbf{p}) = \bar{\pi}(\theta, \mathbf{u}) \mathcal{N}(\rho | 0_d, I_d) \mathcal{N}(\mathbf{p} | 0_D, I_D), \quad (12)$$

which also admits  $\pi(\theta)$  as a marginal. The corresponding equations of motion associated with this extended Hamiltonian are then given by

$$\frac{d}{dt} \begin{pmatrix} \theta \\ \rho \\ \mathbf{u} \\ \mathbf{p} \end{pmatrix} = \begin{pmatrix} \nabla_\theta \log p(\theta) + \nabla_\theta \log \hat{p}(y | \theta, \mathbf{u}) \\ \mathbf{p} \\ -\mathbf{u} + \nabla_\mathbf{u} \log \hat{p}(y | \theta, \mathbf{u}) \end{pmatrix} =: \hat{\Psi}(\theta, \rho, \mathbf{u}, \mathbf{p}). \quad (13)$$

Compared to (7), the intractable log-likelihood gradient  $\nabla_\theta \log p(y | \theta)$  appearing in (7) has now been replaced by the gradient  $\nabla_\theta \log \hat{p}(y | \theta, \mathbf{u})$  of the log-simulated likelihood  $\hat{p}(y | \theta, \mathbf{u})$  where  $\mathbf{u}$  evolves according to the third and fourth rows of (13).

*Remark.* The normality assumption is not restrictive as we can always generate a uniform random variate from a normal one using the cumulative distribution function of a normal. This assumption has also been used by [8] for the correlated pseudo-marginal MH method and [18] for pseudo-marginal slice sampling. The assumed regularity of the simulated likelihood function  $\hat{p}(y | \theta, \mathbf{u})$  is necessary to implement the pseudo-marginal HMC but limits the range of applications of our methodology. For example, in a state-space model context, the likelihood is usually estimated using a particle filter as in [1] but this results in a discontinuous function  $(\theta, \mathbf{u}) \mapsto \hat{p}(y | \theta, \mathbf{u})$ .

### 2.3 Illustration on latent variable models

Consider the latent variable model described by (2)-(3). In this scenario, the intractable likelihood can be unbiasedly estimated using importance sampling. We introduce an importance density  $q_\theta(x_k | y_k)$  for the latent variable  $X_k$  which we assume can be simulated using  $X_k = \gamma_k(\theta, V)$  where  $\gamma_k : \Theta \times \mathbb{R}^p \rightarrow \mathbb{R}^n$  is a deterministic map and  $V \sim \mathcal{N}(0_p, I_p)$ . We can then approximate the likelihood through

$$\widehat{p}(y_{1:T} | \theta, \mathbf{U}) = \prod_{k=1}^T \widehat{p}(y_k | \theta, \mathbf{U}_k), \quad \text{where} \quad \widehat{p}(y_k | \theta, \mathbf{U}_k) = \frac{1}{N} \sum_{i=1}^N \omega_{\theta,k}(\mathbf{U}_{k,i}), \quad (14)$$

with  $\mathbf{U}_k := (\mathbf{U}_{k,1}, \dots, \mathbf{U}_{k,N})$  and  $\omega_\theta(y_k, \mathbf{U}_{k,i}) = \frac{g_\theta(y_k | X_{k,i}) f_\theta(X_{k,i})}{q_\theta(X_{k,i} | y_k)}$ , where  $X_{k,i} = \gamma_k(\theta, \mathbf{U}_{k,i})$  and  $\mathbf{U}_{k,i} \stackrel{\text{i.i.d.}}{\sim} \mathcal{N}(0_p, I_p)$ . We thus have  $D = TNp$  in this scenario and

$$\nabla_\theta \log \widehat{p}(y_{1:T} | \theta, \mathbf{U}) = \sum_{k=1}^T \sum_{i=1}^N \frac{\omega_\theta(y_k, \mathbf{U}_{k,i})}{\sum_{j=1}^N \omega_\theta(y_k, \mathbf{U}_{k,j})} \nabla_\theta \log \omega_\theta(y_k, \mathbf{U}_{k,i}), \quad (15)$$

$$\nabla_{\mathbf{u}_{k,i}} \log \widehat{p}(y_{1:T} | \theta, \mathbf{U}) = \frac{\omega_\theta(y_k, \mathbf{U}_{k,i})}{\sum_{j=1}^N \omega_\theta(y_k, \mathbf{U}_{k,j})} \nabla_{\mathbf{u}_{k,i}} \log \omega_\theta(y_k, \mathbf{U}_{k,i}). \quad (16)$$

The pseudo-marginal MH algorithm can mix very poorly if the relative variance of the likelihood estimator is large; e.g. if  $N = 1$  in (14). In the pseudo-marginal Hamiltonian dynamics context, the case  $N = 1$  corresponds to an Hamiltonian dynamics on a re-parameterisation of the original joint model and can work well in the absence of multimodality; see e.g. [3]. Thus, we expect pseudo-marginal HMC to be less sensitive to the choice of  $N$  than pseudo-marginal HM; see Section 5 for empirical results.

### 2.4 Convergence results

As  $N$  increases, various results have been established to show that pseudo-marginal MH converges in some sense towards the ‘ideal’ marginal MH; e.g. [2]. For large datasets, it has also been shown that  $N$  should be selected such that the standard deviation of the log-likelihood estimator is around 1 so as to minimize the asymptotic variance of the pseudo-marginal MH averages at fixed computational complexity, see [9, 20].

It is beyond the scope of this paper to establish such precise results for the pseudo-marginal Hamiltonian dynamics and the resulting pseudo-marginal HMC. However, we expect that the pseudo-marginal Hamiltonian dynamics (13) using the simulated likelihood gradient  $\nabla_\theta \log \widehat{p}(y | \theta, \mathbf{U})$  will also converge in some sense towards the ideal Hamiltonian dynamics (7), having access to the exact log-likelihood gradient  $\nabla_\theta \log p(y | \theta)$ , if the variance of  $\nabla_\theta \log \widehat{p}(y | \theta, \mathbf{U}) - \nabla_\theta \log p(y | \theta)$  goes to zero. We establish here a result along those lines. We denote by  $\|\cdot\|$  the Euclidean norm. All proofs are in the appendix.

**Proposition 1.** *Let  $(\theta(t), \rho(t))$  be the flow associated to the ideal Hamiltonian dynamics (7) and  $(\widehat{\theta}(t), \widehat{\rho}(t))$  be the flow of the pseudo-marginal Hamiltonian dynamics (13). If  $(\theta(0), \rho(0)) = (\widehat{\theta}(0), \widehat{\rho}(0)) = (\theta_0, \rho_0)$  where  $(\theta_0, \rho_0) \sim \pi(\theta, \rho)$  and*

$$\Psi(\theta, \rho, \mathbf{u}, \mathbf{p}) := \begin{pmatrix} \rho \\ \nabla_\theta \log p(\theta) + \nabla_\theta \log \widehat{p}(y | \theta) \\ \mathbf{p} \\ -\mathbf{u} + \nabla_{\mathbf{u}} \log \widehat{p}(y | \theta, \mathbf{u}) \end{pmatrix} \quad (17)$$

is Lipschitz with constant  $L$ , then for any  $t \geq 0$

$$\mathbb{E} \left[ \left\| \begin{pmatrix} \hat{\theta}(t) \\ \hat{\rho}(t) \end{pmatrix} - \begin{pmatrix} \theta(t) \\ \rho(t) \end{pmatrix} \right\| \right] \leq \frac{\exp(Lt) - 1}{L} \mathbb{E}_{\theta \sim \pi} \left[ \mathbb{E}_{\mathbf{U} \sim \bar{\pi}(\cdot | \theta)} \left[ \left\| \nabla_{\theta} \log \left( \frac{\hat{p}(y | \theta, \mathbf{U})}{p(y | \theta)} \right) \right\|^2 \right]^{1/2} \right]. \quad (18)$$

We observe that the upper bound (18) is directly related to the second moment of the error in the log-likelihood gradient  $\nabla_{\theta} \log (\hat{p}(y | \theta, \mathbf{U})/p(y | \theta))$  under the stationary regime. The next two propositions establish Central Limit Theorems (CLT) for this error under two asymptotic regimes and show that the second moment of this error converges to the variance as  $N \rightarrow \infty$ .

*Remark.* The Lipschitz assumption on  $\Psi$  will not be satisfied in many practical scenarios and it would be interesting to weaken it. Nevertheless, in the following section we observe experimentally that  $\mathbb{E}[\|\hat{\theta}(t) - \theta(t)\|]$  decreases as the variance of log-likelihood gradient decreases even in scenarios where this assumption is not satisfied.

In the following we assume that  $\theta$  is scalar for notational simplicity. In the multivariate case the results below should be interpreted as holding component-wise. We will denote by  $\mathbb{E}_{\mathcal{N}}[\phi(V)]$  the expectation when  $V$  follows a normal distribution of appropriate dimension. We first investigate the behaviour of the error when the number of data  $T$  is fixed while  $N \rightarrow \infty$ .

**Proposition 2.** *Consider the latent variable model (2)-(3) and  $\nabla_{\theta} \log \hat{p}(y_{1:T} | \theta, \mathbf{U})$  in (15) for a fixed value  $\theta$ . Let  $\varpi_{\theta}(y_k, \mathbf{u}_k) = \omega_{\theta}(y_k, \mathbf{u}_k)/p(y_k | \theta)$  and assume that  $\mathbb{E}_{\mathcal{N}}[\varpi_{\theta}^2(y_k, \mathbf{U}_{k,1})] < \infty$ ,  $\mathbb{E}_{\mathcal{N}}[\{\nabla_{\theta} \varpi_{\theta}(y_k, \mathbf{U}_{k,1})\}^2] < \infty$ , there exist functions  $g_k(\mathbf{u}_{k,1})$  (which may depend on  $\theta$  and  $y_k$ ) such that  $|\nabla_{\theta} \varpi_{\theta}(y_k, \mathbf{U}_{k,1})| \leq g_k(\mathbf{u}_{k,1})$  with  $\mathbb{E}_{\mathcal{N}}[g_k(\mathbf{U}_{k,1})] < \infty$  and  $\mathbb{E}_{\mathcal{N}}[\varpi_{\theta}(y_k, \mathbf{U}_{k,1}) |\nabla_{\theta} \varpi_{\theta}(y_k, \mathbf{U}_{k,1})] < \infty$  for all  $k = 1, \dots, T$ . Then the following CLT holds when  $\mathbf{U} \sim \bar{\pi}(\cdot | \theta)$ :*

$$\sqrt{N} \nabla_{\theta} \log \frac{\hat{p}(y_{1:T} | \theta, \mathbf{U})}{p(y_{1:T} | \theta)} \Rightarrow \mathcal{N}(0, \sigma^2(\theta)) \quad (19)$$

where

$$\sigma^2(\theta) = \sum_{k=1}^T \mathbb{E}_{\mathcal{N}}[\{\nabla_{\theta} \varpi_{\theta}(y_k, \mathbf{U}_{k,1})\}^2]. \quad (20)$$

We obtain the same CLT when  $\mathbf{U} \sim \mathcal{N}(\mathbf{u} | 0_D, I_D)$ . Under additional uniform integrability conditions, see e.g. [23, Section 2.5], the asymptotic mean of  $\sqrt{N} \nabla_{\theta} \log (\hat{p}(y | \theta, \mathbf{U})/p(y | \theta))$  converges (unsurprisingly) to zero while its variance converges to  $\sigma^2(\theta)$ .

Next we consider the case when  $N$  scales with  $T$ . Specifically, we present a result below that shows that a conditional CLT holds when  $N = \lceil \beta T \rceil$  for some  $\beta > 0$  and  $T \rightarrow \infty$ . Here  $\mathcal{F}^T$  denotes the sigma-algebra spanned by  $Y_{1:T}$ .

**Proposition 3.** *Consider the latent variable model (2)-(3) and  $\nabla_{\theta} \log \hat{p}(y_{1:T} | \theta, \mathbf{U})$  in (15) for a fixed value  $\theta$ . Assume  $N = \lceil \beta T \rceil$  with  $\beta > 0$ ,  $Y_t \stackrel{i.i.d.}{\sim} \mu$  and  $\mathbf{U} \sim \bar{\pi}(\cdot | \theta)$  then if*

$$\limsup_T \mathbb{E}[(\nabla_{\theta} \varepsilon_N(Y_T; \mathbf{U}_T; \theta))^4] < \infty, \quad \limsup_T \mathbb{E}[(\varepsilon_N(Y_T, \mathbf{U}_T; \theta))^4] < \infty$$

where  $\varepsilon_N(Y_k, \mathbf{U}_k; \theta) := \frac{1}{\sqrt{N}} \sum_{i=1}^N \{\varpi_{\theta}(y_k, \mathbf{U}_{k,i}) - 1\}$ , and conditions to ensure one can swap derivatives and expectations are satisfied, then the following conditional CLT holds as  $T \rightarrow \infty$ :

$$\nabla_{\theta} \log \frac{\hat{p}(Y_{1:T} | \theta, \mathbf{U})}{p(Y_{1:T} | \theta)} \Big| \mathcal{F}^T \Rightarrow \mathcal{N}\left(0, \beta^{-1} \mathbb{E}_{Y_1 \sim \mu, \mathbf{U}_{1,1} \sim \mathcal{N}(0_p, I_p)} [\{\nabla_{\theta} \varpi_{\theta}(Y_1, \mathbf{U}_{1,1})\}^2]\right). \quad (21)$$

This result is surprising as it shows that, under an additional uniform integrability assumption,  $\nabla_\theta \log \hat{p}(y_{1:T} | \theta, \mathbf{U})$  is asymptotically an *unbiased* estimate of  $\nabla_\theta \log p(y_{1:T} | \theta)$  under this regime. When  $\mathbf{U} \sim \mathcal{N}(\mathbf{u} | 0_D, I_D)$ , this asymptotic unbiasedness property does not hold.

*Remark.* The CLT above provide insights on how the number of samples  $N$  needs to be scaled with  $T$  to maintain a certain level of accuracy in the estimate of the log-likelihood gradient as  $T$  becomes large. However, it should be noted that in practice this scaling might still not be the most appropriate choice when taking computational cost into account. The reason is that the pseudo-marginal HMC algorithm does not “break down” in the same way as pseudo-marginal Metropolis-Hastings when using a small  $N$  relative to  $T$ . Indeed, as pointed out above, even the case  $N = 1$  can result in a pseudo-marginal HMC with good performance in some cases, since the method then simply reduces to a standard HMC on the joint space. Intuitively, based on the convergence results presented above, increasing  $N$  can be seen as a way of gradually moving from an HMC sampling on the joint space to an HMC sampling on the marginal space. Thus, in practice, the choice of  $N$  for pseudo-marginal HMC is a tuning parameter that needs to be selected based on the properties of the target posterior.

## 2.5 Numerical illustration

To investigate the behaviour of the pseudo-marginal Hamiltonian system (13) as  $N$  increases, we consider a simple hierarchical Gaussian model with  $d = \dim(\theta) = 1$  and  $T = 30$  latent variables/observations. Let  $p(\theta) = \mathcal{N}(\theta; 0, \sigma_0^2)$  be the prior for  $\theta$  and let  $X_k \stackrel{\text{i.i.d.}}{\sim} \mathcal{N}(\theta, \sigma_1^2)$  and  $Y_k | (X_k = x_k) \sim \mathcal{N}(x_k, \sigma_2^2)$  for  $k = 1, \dots, T$ . The posterior density  $\pi(\theta) = p(\theta | y_{1:T})$  is a normal and available in closed form. The Hamiltonian dynamics (7) is thus described by a harmonic oscillator and denoted  $(\theta(t), \rho(t))$ , with an initial condition  $(\theta_0, \rho_0)$ .

The pseudo-marginal Hamiltonian system relies on the likelihood estimator  $\hat{p}(y_{1:T} | \theta, \mathbf{U})$  defined by (14). We use as importance density the prior  $q_\theta(x_k | y_k) = f_\theta(x_k) = \mathcal{N}(x_k; \theta, \sigma_1^2)$ . We have  $X_{k,i} \sim f_\theta(\cdot)$  if  $X_{k,i} = \theta + \sigma_1 \mathbf{U}_{k,i}$  with  $\mathbf{U}_{k,i} \sim \mathcal{N}(0, 1)$ . We generate a batch of data  $y_{1:T}$  from the system with  $\sigma_0^2 = 10$ ,  $\sigma_1^2 = 0.1$ ,  $\sigma_2^2 = 1$  and simulate (13), denoting the solution by  $(\hat{\theta}^N(t), \hat{\rho}^N(t), \hat{\mathbf{u}}^N(t), \hat{\mathbf{p}}^N(t))$ , for a few randomly selected initial conditions. The maximal error over the integration interval  $[0, 1]$  for different values of  $N$  are reported in Figure 1. Figure 2 show the simulated trajectories for varying initial conditions for the auxiliary variables, for  $N = 1$  and  $N = 50$ . The numerical results indicate a  $\sqrt{N}$  convergence in  $\sup_{t \in [0,1]} |\theta(t) - \hat{\theta}^N(t)|$ .

## 3 Pseudo-marginal Hamiltonian Monte Carlo

The pseudo-marginal Hamiltonian dynamics (13) can not in general be solved analytically and, as usual, we therefore need to make use of a numerical integrator. The standard choice in HMC is to use the Verlet scheme [14, Section 2.2] which is a symplectic integrator of order  $O(h^2)$ , where  $h$  is the integration step-size. However, the error of the Verlet integrator will also depend on the dimension of the system. For the pseudo-marginal target density (12), we therefore need to take the effect of the  $D$ -dimensional auxiliary variable  $\mathbf{u}$  into account. For instance, in the context of importance-sampling-based pseudo-marginal HMC for latent variable models of Section 2.3, we have  $D = TNp$ , i.e. the dimension of the extended target increases linearly with the number  $N$  of importance samples. This is an apparent problem—by increasing  $N$  we expect to obtain solution trajectories closer to those of the true marginal Hamiltonian system, but at the same time the numerical integration error gets amplified.

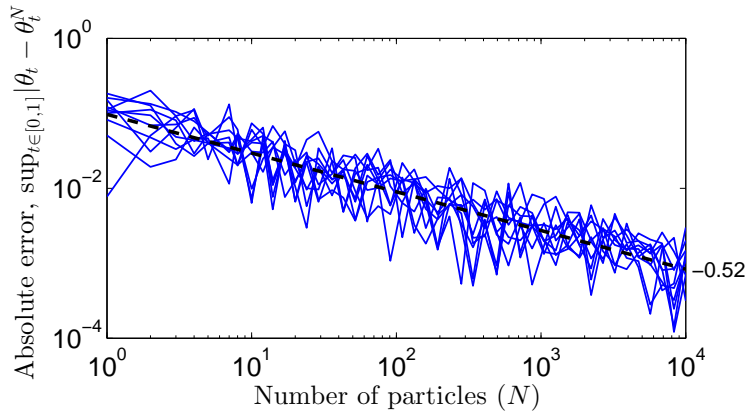


Figure 1:  $\sup_{t \in [0,1]} |\theta(t) - \hat{\theta}^N(t)|$  for different initial conditions. The slope of the linear fit, shown as a dashed line, is  $-0.52$ . (The interval  $[0, 1]$  corresponds to slightly less than one complete period of the marginal system.)

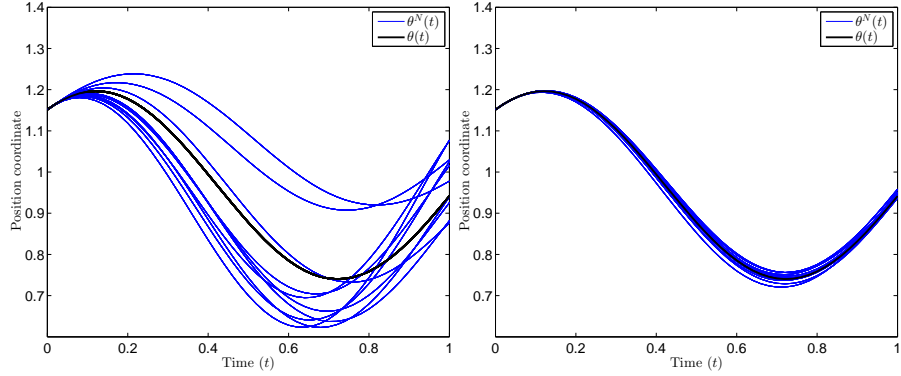


Figure 2: Simulated trajectories  $\hat{\theta}^N(t)$  for  $N = 1$  (left) and for  $N = 50$  (right) in blue, and the trajectory corresponding to the marginal system  $\theta(t)$  (black).

However, it is possible to circumvent this problem by making use of a splitting technique [5],[14, Section 2.4.1], [19, Section 5.5.1] which exploits the structure of the extended target. The idea is to split the Hamiltonian  $H$  defined in (12) into two components  $H = A + B$ , where

$$A(\rho, \mathbf{u}, \mathbf{p}) := \frac{1}{2} \left\{ \rho^T \rho + \mathbf{u}^T \mathbf{u} + \mathbf{p}^T \mathbf{p} \right\}, \quad B(\theta, \mathbf{u}) := -\log p(\theta) - \log \hat{p}(y \mid \theta, \mathbf{u}). \quad (22)$$

The Hamiltonian systems for  $A$  and  $B$  can both be integrated analytically. Indeed, if we define the mapping  $\Phi_t^A : \mathbb{R}^{2d+2D} \mapsto \mathbb{R}^{2d+2D}$  as the solution to the dynamical system with Hamiltonian  $A$  simulated for  $t$  units of time from a given initial condition, we have the explicit solution

$$\Phi_t^A : \begin{cases} \theta(t) = \theta(0) + t\rho(0), \\ \rho(t) = \rho(0), \\ \mathbf{u}(t) = \mathbf{p}(0) \sin(t) + \mathbf{u}(0) \cos(t), \\ \mathbf{p}(t) = \mathbf{p}(0) \cos(t) - \mathbf{u}(0) \sin(t). \end{cases}$$

Similarly for system  $B$  we get,

$$\Phi_t^B : \begin{cases} \theta(t) = \theta(0), \\ \rho(t) = \rho(0) + t\nabla_\theta \{\log p(\theta) + \nabla_\theta \log \hat{p}(y \mid \theta, \mathbf{u}(0))\}_{\theta=\theta(0)}, \\ \mathbf{u}(t) = \mathbf{u}(0), \\ \mathbf{p}(t) = \mathbf{p}(0) + t\nabla_\mathbf{u} \log \hat{p}(y \mid \theta(0), \mathbf{u})_{\mathbf{u}=\mathbf{u}(0)}. \end{cases}$$

Let the integration time be given as  $hL$ , where  $h$  is the step-size and  $L$  an integer. To approximate the solution to the original system associated to the vector field  $\hat{\Psi}$  in (13), we then use a symmetric Strang splitting (see e.g., [14, p. 108]) defined as  $\hat{\Phi}_{hL} = \{\Phi_{A,h/2} \circ \Phi_{B,h} \circ \Phi_{A,h/2}\}^{\circ L}$ . An alternative method which also exploits the structure of the extended Hamiltonian and that could be used in our setting is the exponential integration technique of [7]. In simulations we found the two integrators to perform similarly, however, and we focus on the splitting technique for simplicity. The proposed pseudo-marginal HMC algorithm is summarized in Algorithm 1.

---

**Algorithm 1** Pseudo-marginal HMC (one iteration)

---

Let  $(\theta, \mathbf{u})$  be the current state of the Markov chain. Do:

1. Sample  $\rho \sim \mathcal{N}(0_d, I_d)$  and  $\mathbf{p} \sim \mathcal{N}(0, I_D)$ .
2. Compute  $(\theta', \rho', \mathbf{u}', \mathbf{p}') = \hat{\Phi}_{hL}(\theta, \rho, \mathbf{u}, \mathbf{p})$ .
3. Accept  $(\theta', \mathbf{u}')$  with probability  $1 \wedge \exp(H(\theta, \rho, \mathbf{u}, \mathbf{p}) - H(\theta', \rho', \mathbf{u}', \mathbf{p}'))$ .

---

## 4 Numerical Illustrations

We illustrate the proposed pseudo-marginal HMC (PM-HMC) method on two synthetic examples. Additional details and results are given in the appendix.

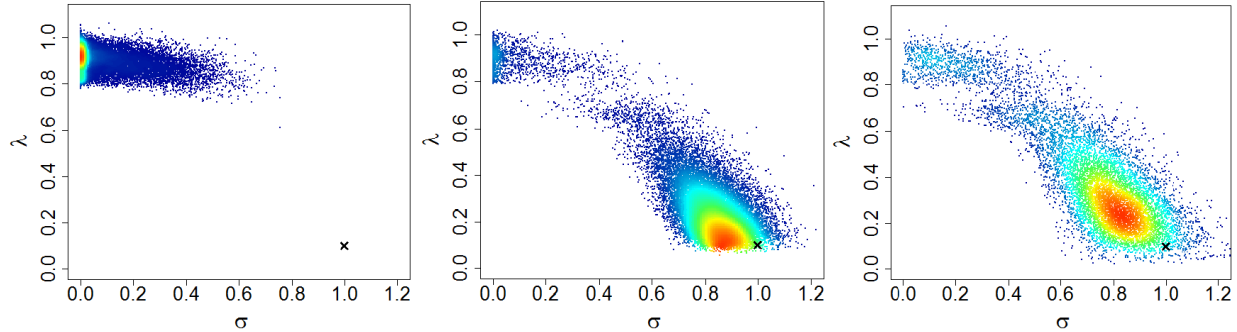


Figure 3: Scatter plots and marginal histograms for  $(\sigma, \lambda)$  for standard HMC, using a non-centered parameterisation (left), PM-HMC with  $N = 16$  (mid), and pseudo-marginal slice sampling with  $N = 128$  (right).

#### 4.1 Diffraction model

Consider a hierarchical model of the form,  $X_k \mid \theta \stackrel{\text{i.i.d.}}{\sim} \mathcal{N}(\mu, \sigma^2)$  and  $Y_k \mid (X_k = x_k), \theta \sim g(\cdot \mid x_k, \lambda)$ , with  $\theta = (\mu, \log(\sigma), \log(\lambda))$ , where the observation density is modelled as a diffraction intensity:  $g(y \mid x, \lambda) = (\lambda\pi)^{-1} \text{sinc}^2(\lambda^{-1}(y - x))$ . We simulate  $T = 100$  i.i.d. observations using  $\mu = 1$ ,  $\sigma = 1$ , and  $\lambda = 0.1$ . We apply the PM-HMC with  $N$  ranging from 16 to 256, using a non-centered parameterization and the prior as importance density, as well as a standard HMC working on the joint space (equivalent to PM-HMC with  $N = 1$ ) using the same non-centered parameterization. For further comparison we also ran, (i) a standard pseudo-marginal MH algorithm using  $N = 512$  and  $N = 1024$  (smaller  $N$  resulted in very sticky behaviour), (ii) the pseudo-marginal slice sampler by [18] with  $N$  ranging from 16 to 256, and (iii) a Gibbs sampler akin to the Particle Gibbs algorithm by [1] (using independent conditional importance sampling kernels to update the latent variables).

Figure 3 shows scatter plots from 40 000 iterations (after a burn-in of 10 000) for the parameters  $(\sigma, \lambda)$  for standard HMC, PM-HMC ( $N = 16$ ), and pseudo-marginal slice sampling ( $N = 128$ , smaller values gave very poor mixing). Results for the remaining methods/settings, including the pseudo-marginal MH method and the Particle Gibbs sampler which both performed very poorly, are given in the appendix.

It is clear that HMC fails to explore the distribution due to the raggedness of the joint posterior. PM-HMC effectively marginalizes out the multimodal latent variables and effectively samples the marginal posterior which, albeit still bimodal, is much smoother than the joint posterior. Pseudo-marginal slice sampling also does well in this example and we found the two methods to be comparable in performance when normalized by computational cost.<sup>2</sup>

#### 4.2 Generalized linear mixed model

Next, we consider inference in a generalized linear mixed model (GLMM, see e.g. [24]) with a logistic link function:  $Y_{ij} \sim \text{Bernoulli}(p_{ij})$ , where  $\text{logit}(p_{ij}) = X_i + Z_{ij}^T \beta$  for  $i = 1:T$ ,  $j = 1:n_i$ . Here,  $Y_{ij}$  represent the  $j$ th observation for the  $i$ th ‘‘subject’’,  $Z_{ij}$  is a covariate of dimension  $p$ ,  $\beta$  is a vector of fixed effects and  $X_i$  is a random effect for subject  $i$ . It has been recognized [6, 13] that it is

<sup>2</sup>We do not report effective sample size estimates, as we found these to be very noisy and misleading for this multimodal distribution. Indeed, the ‘‘best’’ effective sample size when normalized by computational cost was obtained for the Particle Gibbs sampler which, by visual inspection, completely failed to converge to the correct posterior.

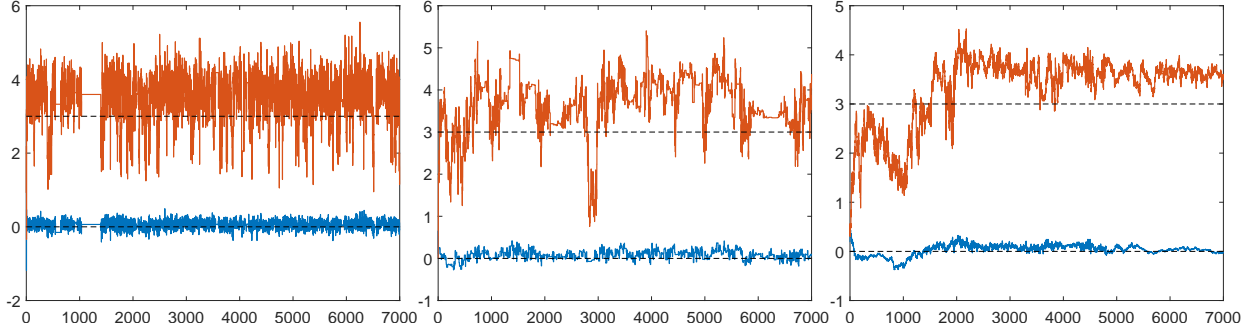


Figure 4: Traces for parameters  $\mu_1$  and  $\mu_2$  for PM-HMC (left), pseudo-marginal slice sampling (mid), and Particle Gibbs sampling (right), all with  $N = 128$ .

often beneficial to allow for non-Gaussianity in the random effects. For instance, multi-modality can arise as an effect of under-modelling, when effects not accounted for by the covariates result in a clustering of the subjects. To accommodate this we assume  $X_i$  to be distributed according to a Gaussian mixture:  $X_i \stackrel{\text{i.i.d.}}{\sim} \sum_{j=1}^K w_j \mathcal{N}(\mu_j, \lambda_j^{-1})$ . For simplicity we fix  $K = 2$  for this illustration. The parameters of the model are thus  $\beta$ ,  $\{\mu_j, \lambda_j\}_{j=1}^2$ , and  $w_1$  (as  $w_2 = 1 - w_1$ ), with  $X_{1:T}$  being latent variables. We use the parameterisation

$$\theta = (\beta^T, \mu_1, \mu_2, \log(\lambda_1), \log(\lambda_2), \text{logit}(w_1))^T \in \mathbb{R}^{p+5}.$$

We used a simulated data set with  $T = 500$  and  $n_i \equiv 6$ , thus a total of 3 000 data points, with  $\mu_1 = 0$ ,  $\mu_2 = 3$ ,  $\lambda_1 = 10$ ,  $\lambda_2 = 3$ . We set  $p = 8$  and generate  $\beta$  as well the covariates  $Z_{ij}$  from standard normal distributions (see the appendix for further details on the simulation setup).

We ran PM-HMC, pseudo-marginal slice sampling [18], and Particle Gibbs [1] for 7 000 iterations, all using  $N = 128$ . We note that Gibbs sampling type algorithms (of which our Particle Gibbs sampler is an example) are the *de facto* standard methods for Bayesian GLMMs. Figure 4 shows traces for the parameters  $\mu_1$  and  $\mu_2$ , with additional results reported in the appendix. The PM-HMC method clearly outperforms the competing methods in terms of mixing (the computational cost per iteration is about 3.5 times higher for PM-HMC than for pseudo-marginal slice sampling in our implementation). In particular, compared to the results of Section 4.1, we note that PM-HMC handles this more challenging model with a 13-dimensional  $\theta$  much better than the pseudo-marginal slice sampling which appears here to struggle for high-dimensional  $\theta$ .

However, we also note that the pseudo-marginal HMC algorithm gets stuck for quite many iterations around iteration 1 000 (see Figure 4). Experiments suggest that this stickiness is an issue inherited from the marginal HMC (which pseudo-marginal HMC approximates) and is not specific to the pseudo-marginal HMC algorithm. Specifically, we have experienced that the pseudo-marginal HMC sampler tends to get stuck at large values of  $\lambda_1$  or  $\lambda_2$ , i.e., in the right tail of the posterior for one of these parameters. A potential solution to address this issue is to use a state-dependent mass matrix as in the Riemannian manifold HMC [12].

## 5 Discussion

HMC methods cannot be implemented in scenarios where the likelihood function is intractable. However, we have shown here that if we have access to a non-negative unbiased likelihood estimator

parameterized by normal random variables then it is possible to derive an algorithm which mimics the HMC algorithm having access to the exact likelihood. The resulting pseudo-marginal HMC algorithm replaces the original intractable gradient of the log-likelihood by the gradient of the log-likelihood estimator while preserving the target distribution as invariant distribution. Empirically we have observed that this algorithm can work significantly better than the pseudo-marginal MH algorithm as well as the standard HMC method sampling on the joint space for a fixed computational budget.

However, whereas clear guidelines are available for optimizing the performance of the pseudo-marginal MH algorithm [9, 20], it is unclear how to address this problem for the pseudo-marginal HMC method. As we increase the number of samples  $N$ , the pseudo-marginal HMC algorithm can be seen as moving from an HMC sampling on the joint space (using a non-centered parameterization) to an HMC sampling on the marginal space. Thus, even the case  $N = 1$  results in a method which, in some cases, works well even for large  $T$ —we do not experience the same “break down” of the method as for pseudo-marginal MH when using a too small  $N$  relative to  $T$ . In practice the number of samples  $N$  is therefore a tuning parameter that needs to be chosen based on the geometry of the target posterior and traded off with the computational cost of the method.

Finally, we have restricted ourselves here for presentation brevity to the pseudo-marginal approximation of a standard HMC algorithm using a constant mass matrix and a Verlet scheme. However, it is clear that the same ideas can be straightforwardly extended to more sophisticated HMC schemes such as the Riemannian manifold HMC [12] or schemes discretizing the associated Nosé-Hoover dynamics described in the appendix.

## Acknowledgments

Arnaud Doucet’s research is supported by the UK Engineering and Physical Sciences Research Council, grants EP/K000276/1 and EP/K009850/1. Fredrik Lindsten’s research is supported by the Swedish Research Council (VR) via the project *Learning of complex dynamical systems* (Contract number: 637-2014-466).

## References

- [1] C. Andrieu, A. Doucet and R. Holenstein. Particle Markov chain Monte Carlo methods (with Discussion). *Journal of the Royal Statistical Society, Series B* **72**, 269–342, 2010.
- [2] C. Andrieu and G.O. Roberts. The pseudo-marginal approach for efficient Monte Carlo computations. *The Annals of Statistics* **37**, 697–725, 2009.
- [3] M. Betancourt and M. Girolami. Hamiltonian Monte Carlo for hierarchical models. in *Current Trends in Bayesian Methodology with Applications*, 79–101, CRC Press, 2015.
- [4] M. Beaumont. Estimation of population growth or decline in genetically monitored populations. *Genetics* **164**, 1139–1160, 2003.
- [5] A. Beskos, F.J. Pinski, J.M. Sanz-Serna and A.M. Stuart. Hybrid Monte Carlo on Hilbert spaces. *Stochastic Processes and their Applications*, **121**, 2201–2230, 2011.
- [6] M. Burda, M. Harding and J. Hausman. A Bayesian mixed logit–probit model for multinomial choice. *Journal of Econometrics* **147**, 232–246, 2008.

- [7] W.L. Chao, J. Solomon, D.L. Michels and F. Sha. Exponential integration for Hamiltonian Monte Carlo. in *Proceedings of the 32nd International Conference on Machine Learning*, 2015.
- [8] G. Deligiannidis, A. Doucet and M.K. Pitt. The correlated pseudo-marginal method. arXiv:1511.04992v3, 2015.
- [9] A. Doucet, M.K. Pitt, G. Deligiannidis and R. Kohn. Efficient implementation of Markov chain Monte Carlo when using an unbiased likelihood estimator. *Biometrika* **102**, 295-313, 2015.
- [10] S. Duane, A.D. Kennedy, B.J. Pendleton and D. Roweth. Hybrid Monte Carlo. *Physics Letters B*, 195(2), 216-222, 1987.
- [11] T. Flury and N. Shephard. Bayesian inference based only on simulated likelihood: particle filter analysis of dynamic economic models. *Econometric Theory* **27**:933–956, 2011.
- [12] M. Girolami and B. Calderhead. Riemann manifold Langevin and Hamiltonian Monte Carlo methods. *Journal of the Royal Statistical Society: Series B* **73**:1-37, 2011.
- [13] A. Komárek and E. Lesaffre. Generalized linear mixed model with a penalized Gaussian mixture as a random effects distribution. *Computational Statistics and Data Analysis* **52**, 3441-3458, 2008.
- [14] B.J. Leimkuhler and C. Matthews. *Molecular Dynamics with Deterministic and Stochastic Numerical Methods*, Springer, 2015.
- [15] B. Leimkuhler and S. Reich. A Metropolis adjusted Nosé-Hoover thermostat. *ESAIM: Mathematical Modelling and Numerical Analysis* **43**, 743-755, 2009.
- [16] L. Lin, K.F. Liu and J. Sloan. A noisy Monte Carlo algorithm. *Physical Review D* **61**, 074505, 2010.
- [17] E. Meeds, R. Leenders and M. Welling. Hamiltonian ABC. In *Proceedings of the 31st conference on Uncertainty in Artificial Intelligence*, 2015.
- [18] I. Murray and M.M. Graham. Pseudo-marginal slice sampling. *Proceedings of the 19th International Conference on Artificial Intelligence and Statistics*, 2016.
- [19] R.M. Neal, MCMC using Hamiltonian dynamics. in *Handbook of Markov chain Monte Carlo*, 113-162, CRC Press, 2011.
- [20] C. Sherlock, A. Thiery, G.O. Roberts and J.S. Rosenthal. On the efficiency of pseudo-marginal random walk Metropolis algorithms. *The Annals of Statistics* **43**, 238–275, 2015.
- [21] H. Strathmann, D. Sejdinovic, S. Livingstone, Z. Szabo and A. Gretton. Gradient-free Hamiltonian Monte Carlo with efficient kernel exponential families. In *Advances in Neural Information Processing Systems*, 2015.
- [22] K.E. Train. *Discrete Choice Methods with Simulation*. Cambridge University Press, 2009.
- [23] A.W. van der Vaart. *Asymptotic Statistics*. Cambridge University Press, 2000.
- [24] Y. Zhao, J. Staudenmayer, B.A. Coull and M.P. Wand. General design Bayesian generalized linear mixed models. *Statistical Science*, 35-51, 2006.

## A Convergence of Hamiltonian dynamics

We first establish a preliminary proposition which shows how one can bound the norm of the difference between the solutions of two ordinary differential equations. This result follows from a slight modification of Grönwall's lemma. We denote by  $\|\cdot\|$  the Euclidean norm.

**Proposition 4.** *Let  $f, \hat{f} : \mathbb{R}^n \rightarrow \mathbb{R}^n$  be continuous functions and let  $x, \hat{x} : [0, T] \rightarrow \mathbb{R}^n$  satisfy the initial value problems*

$$\frac{dx}{dt} = f(x), \quad \frac{d\hat{x}}{dt} = \hat{f}(\hat{x}), \quad (23)$$

with  $x(0) = \hat{x}(0)$ . If  $f$  is Lipschitz with constant  $L$ , i.e. for any  $x_1, x_2$

$$\|f(x_1) - f(x_2)\| \leq L\|x_1 - x_2\| \quad (24)$$

then for any  $t \geq 0$

$$\|\hat{x}(t) - x(t)\| \leq \exp(Lt) \int_0^t \exp(-Ls)\varepsilon(\hat{x}(s))ds. \quad (25)$$

where

$$\varepsilon(x) := \|\hat{f}(x) - f(x)\|. \quad (26)$$

*Proof.* For any differentiable function  $z : [0, T] \rightarrow \mathbb{R}^n$ , it follows from Cauchy-Schwartz inequality that

$$\frac{d\|z\|}{dt} = \|z\|^{-1} \left( \frac{dz}{dt} \right)^T z \leq \left\| \frac{dz}{dt} \right\|.$$

Hence, we have

$$\begin{aligned} \frac{d\|\hat{x} - x\|}{dt} &\leq \left\| \frac{d\hat{x}}{dt} - \frac{dx}{dt} \right\| \\ &= \|\hat{f}(\hat{x}(t)) - f(x(t))\| \\ &\leq \|f(\hat{x}(t)) - f(x(t))\| + \|\hat{f}(\hat{x}(t)) - f(\hat{x}(t))\| \\ &\leq L\|\hat{x}(t) - x(t)\| + \varepsilon(\hat{x}(t)) \end{aligned}$$

by the triangular inequality, (24) and (26) so

$$\frac{d\|\hat{x} - x\|}{dt} - L\|\hat{x}(t) - x(t)\| \leq \varepsilon(\hat{x}(t)).$$

By multiplying by  $\exp(-Lt)$ , one obtains

$$\frac{d}{dt}(\exp(-Lt)\|\hat{x}(t) - x(t)\|) \leq \exp(-Lt)\varepsilon(\hat{x}(t)). \quad (27)$$

The result (25) follows by integrating (27) from 0 to  $t$  and using  $x(0) = \hat{x}(0)$ .  $\square$

At first sight, this result might appear of limited interest as the upper bound in the r.h.s. of (25) depends on  $\hat{x}(t)$ . However, in our context, we will be able to exploit the following corollary.

**Corollary 1.** Assume there exists a probability density  $\mu$  such that

$$\nabla \cdot (\hat{f}\mu) = \sum_{i=1}^n \partial_{x_i} \left\{ \hat{f}_i(x)\mu(x) \right\} = 0 \quad (28)$$

and  $\hat{x}(0) = x(0) := X_0 \sim \mu$  then, for any  $t \geq 0$ ,  $\hat{x}(t) \sim \mu$  and

$$\mathbb{E}[\|\hat{x}(t) - x(t)\|] \leq \frac{\exp(Lt) - 1}{L} \mathbb{E}_\mu[\varepsilon(X_0)].$$

*Proof.* Condition (28) ensures that  $\hat{f}$  defines a flow preserving the measure  $\mu$  so that  $\hat{x}(t) \sim \mu$  (see e.g. [14, Section 5.2.2]) and, using (25), we obtain

$$\begin{aligned} \mathbb{E}_{X_0 \sim \mu}[\|\hat{x}(t) - x(t)\|] &\leq \exp(Lt) \int_0^t \exp(-Ls) \mathbb{E}_{X_0 \sim \mu}[\varepsilon(\hat{x}(s))] ds \\ &= \exp(Lt) \mathbb{E}_{X_0 \sim \mu}[\varepsilon(X_0)] \int_0^t \exp(-Ls) ds \\ &= \frac{\exp(Lt) - 1}{L} \mathbb{E}_{X_0 \sim \mu}[\varepsilon(X_0)] \end{aligned}$$

where we have used Fubini and  $\mathbb{E}_{X_0 \sim \mu}[\varepsilon(\hat{x}(t))] = \mathbb{E}_{X_0 \sim \mu}[\varepsilon(X_0)]$ .  $\square$

We are now in a position to prove Proposition 1.

*Proof of Proposition 1.* We want to apply here Proposition 4 but it is not possible to compare directly the vector field  $\varphi$  in (8) of the ideal HMC to the vector field  $\hat{\Psi}$  in (13) of the pseudo-marginal HMC as they are defined on different spaces. Hence, we augment  $\varphi$  to obtain  $\Psi$  in (17). We note that, under  $\Psi$ ,  $(\theta(t), \rho(t))$  still evolve according to the ideal HMC dynamics while, for a fixed  $\theta$ , the two last components  $(\mathbf{u}(t), \mathbf{p}(t))$  preserve  $\bar{\pi}(\mathbf{u}|\theta)\mathcal{N}(\mathbf{p}; 0_D, I_D)$  invariant (note however that  $\Psi$  does not correspond to a Hamiltonian dynamical system). Now we have

$$\left\| \hat{\Psi}(\theta, \rho, \mathbf{u}, \mathbf{p}) - \Psi(\theta, \rho, \mathbf{u}, \mathbf{p}) \right\| = \left| \nabla_\theta \log \left( \frac{\hat{p}(y \mid \theta, \mathbf{u})}{p(y \mid \theta)} \right) \right|.$$

As we have assumed that  $\Psi$  is Lipschitz and since  $\hat{\Psi}$  preserves the extended target  $\bar{\pi}(\theta, \rho, \mathbf{u}, \mathbf{p})$  given in (12) by construction, we can use Proposition 4 and Corollary 1 to obtain

$$\begin{aligned} \mathbb{E} \left[ \left\| \begin{pmatrix} \hat{\theta}(t) \\ \hat{\rho}(t) \end{pmatrix} - \begin{pmatrix} \theta(t) \\ \rho(t) \end{pmatrix} \right\| \right] &\leq \mathbb{E} \left[ \left\| \begin{pmatrix} \hat{\theta}(t) \\ \hat{\rho}(t) \\ \hat{\mathbf{u}}(t) \\ \hat{\mathbf{p}}(t) \end{pmatrix} - \begin{pmatrix} \theta(t) \\ \rho(t) \\ \mathbf{u}(t) \\ \mathbf{p}(t) \end{pmatrix} \right\| \right] \\ &\leq \frac{\exp(Lt) - 1}{L} \mathbb{E}_{\bar{\pi}} \left[ \left| \nabla_\theta \log \left( \frac{\hat{p}(y \mid \theta, \mathbf{U})}{p(y \mid \theta)} \right) \right| \right]. \end{aligned}$$

By iterated expectation and Jensen's we obtain

$$\begin{aligned} \mathbb{E}_{\bar{\pi}} \left[ \left| \nabla_\theta \log \left( \frac{\hat{p}(y \mid \theta, \mathbf{U})}{p(y \mid \theta)} \right) \right| \right] &= \mathbb{E}_{\theta \sim \pi} \left[ \mathbb{E}_{\mathbf{U} \sim \bar{\pi}(\cdot \mid \theta)} \left[ \left| \nabla_\theta \log \left( \frac{\hat{p}(y \mid \theta, \mathbf{U})}{p(y \mid \theta)} \right) \right| \right] \right] \\ &\leq \mathbb{E}_{\theta \sim \pi} \left[ \mathbb{E}_{\mathbf{U} \sim \bar{\pi}(\cdot \mid \theta)} \left[ \left\{ \nabla_\theta \log \left( \frac{\hat{p}(y \mid \theta, \mathbf{U})}{p(y \mid \theta)} \right) \right\}^2 \right]^{1/2} \right] \end{aligned}$$

and the result follows.  $\square$

## B Proofs of the Central Limit Theorems

*Proof of Proposition 2.* We first prove the result for  $\mathbf{U} \sim \mathcal{N}(0_D, I_D)$  then the result for  $\mathbf{U} \sim \bar{\pi}(\cdot | \theta)$  follows from a perturbation argument. We have

$$\begin{aligned} & \log \hat{p}(y_{1:T} | \theta, \mathbf{U}) - \log p(y_{1:T} | \theta) \\ &= \sum_{k=1}^T \log \left\{ 1 + \frac{\hat{p}(y_k | \theta, \mathbf{U}_k) - p(y_k | \theta)}{p(y_k | \theta)} \right\} \\ &= \sum_{k=1}^T \log \left\{ 1 + \frac{\varepsilon_N(Y_k, \mathbf{U}_k; \theta)}{\sqrt{N}} \right\} \end{aligned}$$

where

$$\varepsilon_N(Y_k, \mathbf{U}_k; \theta) := \sqrt{N} \frac{\hat{p}(y_k | \theta, \mathbf{U}_k) - p(y_k | \theta)}{p(y_k | \theta)} = \frac{1}{\sqrt{N}} \sum_{i=1}^N \{\varpi_\theta(y_k, \mathbf{U}_{k,i}) - 1\}. \quad (29)$$

Hence, we have

$$\sqrt{N} \{ \nabla_\theta \log \hat{p}(y_{1:T} | \theta, \mathbf{U}) - \nabla_\theta \log p(y_{1:T} | \theta) \} = \sum_{k=1}^T \frac{\nabla_\theta \varepsilon_N(y_k, \mathbf{U}_k; \theta)}{1 + \varepsilon_N(y_k, \mathbf{U}_k; \theta) / \sqrt{N}}. \quad (30)$$

As  $\mathbb{E}_N[\varepsilon_N(y_k, \mathbf{U}_k; \theta)^2] = \mathbb{E}_N[\varpi_\theta(y_k, \mathbf{U}_{k,1})^2] - 1 < \infty$  by assumption then if  $\mathbf{U} \sim \mathcal{N}(0_D, I_D)$ , we have  $\varepsilon_N(y_k, \mathbf{U}_k; \theta) / \sqrt{N} \rightarrow 0$  in probability by Chebyshev's inequality. Hence by the continuous mapping theorem, Slutsky's lemma and the standard CLT applied to  $\sum_{k=1}^T \nabla_\theta \varepsilon_N(y_k, \mathbf{U}_k; \theta)$ , the result (19) holds as  $\mathbb{E}_N[\nabla_\theta \varepsilon_N(y_k, \mathbf{U}_k; \theta)] = \sqrt{N} \mathbb{E}_N[\nabla_\theta \varpi_\theta(y_k, \mathbf{U}_{k,1})] = \sqrt{N} \nabla \mathbb{E}_N[\varpi_\theta(y_k, \mathbf{U}_{k,1})] = 0$  given  $|\nabla_\theta \varpi_\theta(y_k, \mathbf{u}_{k,1})| \leq g_k(\mathbf{u}_{k,1})$  with  $\mathbb{E}_N[g_k(\mathbf{U}_{k,1})] < \infty$ .

Now if  $\mathbf{U} \sim \bar{\pi}(\cdot | \theta)$ , we use the fact that  $\bar{\pi}(\mathbf{u} | \theta) = \prod_{k=1}^T \bar{\pi}(\mathbf{u}_k | \theta)$  where

$$\bar{\pi}(\mathbf{u}_k | \theta) = \frac{1}{N} \sum_{j=1}^N \psi_k(\mathbf{u}_{k,j} | \theta) \prod_{i \neq j} \mathcal{N}(\mathbf{u}_{k,i}; 0_p, I_p)$$

and  $\psi_k(\mathbf{u}_{k,1} | \theta) := \mathcal{N}(\mathbf{u}_{k,1}; 0_p, I_p) \times \varpi_\theta(y_k, \mathbf{u}_{k,1})$ . We can sample from  $\bar{\pi}(\mathbf{u}_k | \theta)$  as follows: draw  $J$  uniformly on  $\{1, 2, \dots, N\}$  then draw  $\mathbf{U}_{k,J} \sim \psi_k(\cdot | \theta)$  and draw  $\mathbf{U}_{k,i} \sim \mathcal{N}(0, I_p)$  for  $i \neq J$ . Now introduce a set of variables  $\mathbf{V}_k \sim \mathcal{N}(0, I_{Np})$  and  $\mathbf{V}'_{k,1} \sim \psi_k(\cdot | \theta)$  for  $k = 1, \dots, T$ , then it follows that

$$\begin{aligned} & \text{Law} \left\{ \sqrt{N} \{ \nabla_\theta \log \hat{p}(y_{1:T} | \theta, \mathbf{U}) - \nabla_\theta \log p(y_{1:T} | \theta) \} \right\} \\ &= \text{Law} \left\{ \sum_{k=1}^T \frac{\nabla_\theta \varepsilon_N(y_k, \mathbf{V}_k; \theta) + \frac{1}{\sqrt{N}} (\nabla_\theta \varpi_\theta(y_k, \mathbf{V}'_{k,1}) - \nabla_\theta \varpi_\theta(y_k, \mathbf{V}_{k,1}))}{1 + \frac{1}{\sqrt{N}} \varepsilon_N(y_k, \mathbf{V}_k; \theta) + \frac{1}{N} (\varpi_\theta(y_k, \mathbf{V}'_{k,1}) - \varpi_\theta(y_k, \mathbf{V}_{k,1}))} \right\}. \end{aligned}$$

We have  $\frac{1}{\sqrt{N}} \varepsilon_N(y_k, \mathbf{V}_k; \theta) \rightarrow 0$  and  $\frac{1}{N} \varpi_\theta(y_k, \mathbf{V}_{k,1}) \rightarrow 0$  in probability as  $\mathbb{E}_N[\varpi_\theta(y_k, \mathbf{U}_{k,1})^2] < \infty$  using Chebyshev's inequality and  $\frac{1}{N} \varpi_\theta(y_k, \mathbf{V}'_{k,1}) \rightarrow 0$  in probability because of Markov's inequality and  $\mathbb{E}_{\psi_k}[\varpi_\theta(y_k, \mathbf{V}'_{k,1})] = \mathbb{E}_N[\varpi_\theta(y_k, \mathbf{V}'_{k,1})^2] < \infty$ . Similarly we have  $\frac{1}{\sqrt{N}} \nabla_\theta \varpi_\theta(y_k, \mathbf{V}_{k,1}) \rightarrow 0$  and  $\frac{1}{\sqrt{N}} \nabla_\theta \varpi_\theta(y_k, \mathbf{V}'_{k,1}) \rightarrow 0$  in probability by Chebyshev's and Markov's inequalities since  $\mathbb{E}_N[\{\nabla_\theta \varpi_\theta(y_k, \mathbf{V}_{k,1})\}^2] < \infty$  and  $\mathbb{E}_{\psi_k}[\|\nabla_\theta \varpi_\theta(y_k, \mathbf{V}'_{k,1})\|] < \infty$ . Hence by the continuous mapping theorem and Slutsky's lemma the result follows.  $\square$

*Proof of Proposition 3.* Our proof uses similar techniques as the proof of Theorem 1 in [8] which establishes a CLT for the log-likelihood estimator  $\log \hat{p}(Y_{1:T} | \theta, \mathbf{U})$  as  $T \rightarrow \infty$  when  $N = \lceil \beta T \rceil$ . The random variables  $\{\varepsilon_N(Y_t; \theta)\}_{t=1, \dots, T}$  are conditionally independent given  $\mathcal{F}^T$  under  $\mathbf{U} \sim \bar{\pi}(\cdot | \theta)$  but their distributions depend on  $T$  as  $N = \lceil \beta T \rceil$  so we need to use limit theorems for triangular arrays. We have from (29) and (30)

$$\begin{aligned} \nabla_\theta \log \frac{\hat{p}(Y_{1:T} | \theta, \mathbf{U})}{p(Y_{1:T} | \theta)} &= \sum_{k=1}^T \frac{\nabla_\theta \varepsilon_N(Y_k, \mathbf{U}_k; \theta) / \sqrt{N}}{1 + \varepsilon_N(Y_k, \mathbf{U}_k; \theta) / \sqrt{N}} \\ &= \sum_{k=1}^T \frac{\nabla_\theta \varepsilon_N(Y_k, \mathbf{U}_k; \theta)}{\sqrt{N}} - \frac{\nabla_\theta \varepsilon_N(Y_k, \mathbf{U}_k; \theta) \cdot \varepsilon_N(Y_k, \mathbf{U}_k; \theta)}{N} \\ &\quad + \frac{\nabla_\theta \varepsilon_N(Y_k, \mathbf{U}_k; \theta) \cdot \varepsilon_N(Y_k, \mathbf{U}_k; \theta)^2}{(1 + \xi_N(Y_k; \theta))^3 N \sqrt{N}} \end{aligned} \quad (31)$$

where  $|\xi_N(Y_k; \theta)| \leq |\varepsilon_N(Y_k, \mathbf{U}_k; \theta)| / \sqrt{N}$ . These Taylor expansions need to be valid for  $t \in 1 : T$  so we need to control the event  $B(\mathcal{F}^T, \varepsilon) = \{\max_{k \leq T} |\varepsilon_N(Y_k, \mathbf{U}_k; \theta)| / \sqrt{N} > \varepsilon\}$ . We have for any  $\varepsilon > 0$

$$\begin{aligned} \mathbb{P}(B(\mathcal{F}^T, \varepsilon)) &\leq \sum_{k=1}^T \mathbb{P}\left(\left|\frac{\varepsilon_N(Y_k, \mathbf{U}_k; \theta)}{\sqrt{N}}\right| > \varepsilon\right) = T \mathbb{P}\left(\left|\frac{\varepsilon_N(Y_1, \mathbf{U}_1; \theta)}{\sqrt{N}}\right| > \varepsilon\right) \\ &\leq TN^{-2}\varepsilon^{-4}\mathbb{E}(\varepsilon_N(Y_1, \mathbf{U}_1; \theta)^4) \\ &\rightarrow 0 \text{ as } T \rightarrow \infty. \end{aligned}$$

Hence  $\mathbb{P}(B^C(\mathcal{F}^T, \varepsilon)) \rightarrow 1$  as  $T \rightarrow \infty$ . On the event  $B^C(\mathcal{F}^T, \varepsilon)$ , the Taylor expansion is valid for  $\varepsilon$  small enough and we can write

$$\begin{aligned} &\nabla_\theta \log \hat{p}(Y_{1:T} | \theta, \mathbf{U}) - \nabla_\theta \log p(Y_{1:T} | \theta) \\ &= \sum_{k=1}^T \frac{\nabla_\theta \varepsilon_N(Y_k, \mathbf{U}_k; \theta)}{\beta^{1/2} T^{1/2}} - \frac{\nabla_\theta \varepsilon_N(Y_k, \mathbf{U}_k; \theta) \cdot \varepsilon_N(Y_k, \mathbf{U}_k; \theta)}{\beta T} + \frac{\nabla_\theta \varepsilon_N(Y_k, \mathbf{U}_k; \theta) \cdot \varepsilon_N(Y_k, \mathbf{U}_k; \theta)^2}{(1 + \xi_N(Y_k; \theta))^3 \beta^{3/2} T^{3/2}}. \end{aligned} \quad (32)$$

We have on the event  $B^C(\mathcal{F}^T, \varepsilon)$ , for  $\varepsilon < 1$ ,

$$\begin{aligned} R_n &= \sum_{k=1}^T \frac{|\nabla_\theta \varepsilon_N(Y_k, \mathbf{U}_k; \theta)| \cdot \varepsilon_N(Y_k, \mathbf{U}_k; \theta)^2}{(1 + \xi_N(Y_k; \theta))^3 \beta^{3/2} T^{3/2}} \\ &\leq \frac{1}{(1 - \varepsilon)^3 \beta^{3/2} T^{1/2}} \frac{1}{T} \sum_{k=1}^T |\nabla_\theta \varepsilon_N(Y_k, \mathbf{U}_k; \theta)| \cdot \varepsilon_N(Y_k, \mathbf{U}_k; \theta)^2. \end{aligned}$$

By Hölder's inequality and the assumptions specified in the statement of the proposition, there exists  $\delta > 0$  such that  $\limsup_T \mathbb{E}\left[\left(|\nabla_\theta \varepsilon_N(Y_k, \mathbf{U}_k; \theta)| \cdot \varepsilon_N(Y_k, \mathbf{U}_k; \theta)^2\right)^{1+\delta}\right] < \infty$  so

$$\left(\frac{1}{T} \sum_{k=1}^T |\nabla_\theta \varepsilon_N(Y_k, \mathbf{U}_k; \theta)| \cdot \varepsilon_N(Y_k, \mathbf{U}_k; \theta)^2\right) - \mathbb{E}[|\nabla_\theta \varepsilon_N(Y_1, \mathbf{U}_1; \theta)| \cdot \varepsilon_N(Y_1, \mathbf{U}_1; \theta)^2] \xrightarrow{\mathbb{P}} 0$$

by the weak law of large numbers (WLLN) for triangular arrays and so  $R_n \xrightarrow{\mathbb{P}} 0$ . We now have

$$\sum_{k=1}^T \frac{\nabla_{\theta} \varepsilon_N(Y_k, \mathbf{U}_k; \theta)}{\beta^{1/2} T^{1/2}} = \frac{1}{\beta^{1/2} T^{1/2}} \sum_{k=1}^T \left\{ \nabla_{\theta} \varepsilon_N(Y_k, \mathbf{U}_k; \theta) - \mathbb{E} \left[ \nabla_{\theta} \varepsilon_N(Y_k, \mathbf{U}_k; \theta) \mid \mathcal{F}^T \right] \right\} \quad (33)$$

$$+ \frac{1}{\beta^{1/2} T^{1/2}} \sum_{k=1}^T \mathbb{E} \left[ \nabla_{\theta} \varepsilon_N(Y_k, \mathbf{U}_k; \theta) \mid \mathcal{F}^T \right]. \quad (34)$$

The term on the r.h.s. of (33) satisfies a conditional CLT, as the conditional Lindeberg condition holds because  $\limsup_T \mathbb{E} \left[ \{ \nabla_{\theta} \varepsilon_N(Y_T, \mathbf{U}_T; \theta) \}^4 \right] < \infty$ ; see e.g. Lemma 10 in [8]. The limiting variance is given

$$\begin{aligned} & \lim_{T \rightarrow \infty} \frac{1}{\beta T} \sum_{k=1}^T \left\{ \mathbb{E} \left[ \{ \nabla_{\theta} \varepsilon_N(Y_k, \mathbf{U}_k; \theta) \}^2 \mid \mathcal{F}^T \right] - \mathbb{E}^2 \left[ \nabla_{\theta} \varepsilon_N(Y_k, \mathbf{U}_k; \theta) \mid \mathcal{F}^T \right] \right\} \\ &= \lim_{T \rightarrow \infty} \frac{1}{\beta T} \sum_{k=1}^T \left( 1 - \frac{1}{N} \right) \mathbb{E}_{\mathcal{N}} \left[ \{ \nabla_{\theta} \varpi_{\theta}(Y_k, \mathbf{U}_{k,1}) \}^2 \mid \mathcal{F}^T \right] \\ & \quad + \frac{1}{N} \mathbb{E}_{\mathcal{N}} \left[ \varpi_{\theta}(Y_k, \mathbf{U}_{k,1}) \{ \nabla_{\theta} \varpi_{\theta}(Y_k, \mathbf{U}_{k,1}) \}^2 \mid \mathcal{F}^T \right] \\ & \quad - \left( \frac{1}{2\sqrt{N}} \mathbb{E}_{\mathcal{N}} \left[ \nabla_{\theta} \varpi_{\theta}^2(Y_t, \mathbf{U}_{k,1}) \mid \mathcal{F}^T \right] \right)^2 \\ &= \beta^{-1} \mathbb{E}_{\mathcal{N}} \left[ \{ \nabla_{\theta} \varpi_{\theta}(Y_1, \mathbf{U}_{1,1}) \}^2 \right] \end{aligned}$$

almost surely by the strong law of large numbers (SLLN). To control the second term (34), we note that as  $T \rightarrow \infty$

$$\begin{aligned} \frac{1}{\beta^{1/2} T^{1/2}} \sum_{k=1}^T \mathbb{E} \left[ \nabla_{\theta} \varepsilon_N(Y_k, \mathbf{U}_k; \theta) \mid \mathcal{F}^T \right] &= \frac{1}{2\sqrt{N} \beta^{1/2} T^{1/2}} \sum_{k=1}^T \mathbb{E}_{\mathcal{N}} \left[ \nabla_{\theta} \varpi_{\theta}^2(Y_k, \mathbf{U}_{k,1}) \mid \mathcal{F}^T \right] \\ &\rightarrow \frac{1}{2\beta} \mathbb{E}_{\mathcal{N}} \left[ \nabla_{\theta} \varpi_{\theta}^2(Y_1, \mathbf{U}_{1,1}) \right] \end{aligned} \quad (35)$$

almost surely by the SLLN. Finally by the WLLN for triangular arrays, we have

$$\frac{1}{T} \sum_{k=1}^T \nabla_{\theta} \varepsilon_N(Y_k, \mathbf{U}_k; \theta) \cdot \varepsilon_N(Y_k, \mathbf{U}_k; \theta) - \mathbb{E} [\nabla_{\theta} \varepsilon_N(Y_1, \mathbf{U}_1; \theta) \cdot \varepsilon_N(Y_1, \mathbf{U}_1; \theta)] \xrightarrow{\mathbb{P}} 0$$

as there exists  $\delta > 0$  such that  $\limsup_T \mathbb{E} \left[ |\nabla_{\theta} \varepsilon_N(Y_1, \mathbf{U}_1; \theta) \cdot \varepsilon_N(Y_1, \mathbf{U}_1; \theta)|^{1+\delta} \right] < \infty$  and as  $T \rightarrow \infty$

$$\begin{aligned} & \frac{1}{\beta T} \sum_{t=1}^T \mathbb{E} [\nabla_{\theta} \varepsilon_N(Y_1, \mathbf{U}_1; \theta) \cdot \varepsilon_N(Y_1, \mathbf{U}_1; \theta)] \\ &= \frac{1}{\beta} \left\{ \frac{1}{2} \left( 1 - \frac{1}{N} \right) \mathbb{E}_{\mathcal{N}} \left[ \nabla_{\theta} \varpi_{\theta}^2(Y_1, \mathbf{U}_{1,1}) \right] + \frac{1}{2N} \mathbb{E}_{\mathcal{N}} \left[ \{ \varpi_{\theta}(Y_1, \mathbf{U}_{1,1}) - 1 \} \nabla_{\theta} \varpi_{\theta}^2(Y_1, \mathbf{U}_{1,1}) \right] \right\} \\ &\rightarrow \frac{1}{2\beta} \mathbb{E}_{\mathcal{N}} \left[ \nabla_{\theta} \varpi_{\theta}^2(Y_1, \mathbf{U}_{1,1}) \right]. \end{aligned} \quad (36)$$

We can then conclude by Lemma 11 in [8].  $\square$

## C Extension to Nosé-Hoover dynamics

The Hamiltonian dynamics presented in (7), respectively (13), preserves the Hamiltonian (5), respectively (11). As mentioned earlier, it is thus necessary to randomize periodically the momentum to explore the target distribution of interest. On the contrary, Nosé-Hoover type dynamics do not preserve the Hamiltonian but keep the target distribution of interest invariant [14, Chapter 8]. However, they are not necessarily ergodic but can perform well and it is similarly possible to randomize them to ensure ergodicity.

Compared to the Hamiltonian dynamics (7), the Nosé-Hoover dynamics is given by

$$\frac{d\theta}{dt} = \rho, \quad (37)$$

$$\frac{d\rho}{dt} = \nabla_\theta \log p(\theta) + \nabla_\theta \log p(y | \theta) - \xi\rho, \quad (38)$$

$$\frac{d\xi}{dt} = \mu^{-1}(\rho^T \rho - d) \quad (39)$$

where  $\xi \in \mathbb{R}$  is the so-called thermostat. It is easy to check that this flow preserves

$$\pi(\theta, \rho, \xi) = \pi(\theta, \rho) \mathcal{N}(\xi; 0, \mu^{-1})$$

invariant; i.e. if  $(\theta(0), \rho(0), \xi(0)) \sim \pi$  then  $(\theta(t), \rho(t), \xi(t)) \sim \pi$  for any  $t > 0$ . This dynamics can be straightforwardly extended to the intractable likelihood case to obtain

$$\frac{d\theta}{dt} = \rho, \quad (40)$$

$$\frac{d\rho}{dt} = \nabla_\theta \log p(\theta) + \nabla_\theta \log \hat{p}(y | \theta, \mathbf{u}) - \xi\rho, \quad (41)$$

$$\frac{d\mathbf{u}}{dt} = \mathbf{p}, \quad (42)$$

$$\frac{d\mathbf{p}}{dt} = -\mathbf{u} + \nabla_{\mathbf{u}} \log \hat{p}(y | \theta, \mathbf{u}) - \xi\mathbf{p}, \quad (43)$$

$$\frac{d\xi}{dt} = \mu^{-1}(\rho^T \rho + \mathbf{p}^T \mathbf{p} - (d + D)). \quad (44)$$

This flow preserves

$$\bar{\pi}(\theta, \rho, \mathbf{u}, \mathbf{p}, \xi) = \bar{\pi}(\theta, \rho, \mathbf{u}, \mathbf{p}) \mathcal{N}(\xi; 0, \mu^{-1}).$$

It would also be possible to use the thermostat  $\xi$  to only regulate  $\rho$  as in (37)-(39).

It is possible to combine Nosé-Hoover numerical integrators with an MH accept-reject step to preserve the invariant distribution [15]. A weakness of this approach is that the MH accept-reject step is not only dependent of the difference between the ratio of the target at the proposed state and the target at the initial state but involves an additional Jacobian factor. We will not explore further these approaches here, which will be the subject of future work.

## D Details about the numerical illustrations and additional results

### D.1 Diffraction model

A normal  $\mathcal{N}(0, 10^2)$  prior was used for each component of  $\theta$ . We used  $h = 0.02$  and  $L = 50$  in all cases for simplicity, resulting in average acceptance probabilities in the range 0.6–0.8.

In Figures 5–9 below we show traces for the parameter  $\lambda$  (which, along with  $\sigma$ , was the most difficult parameter to infer) for the various samplers considered with different settings.

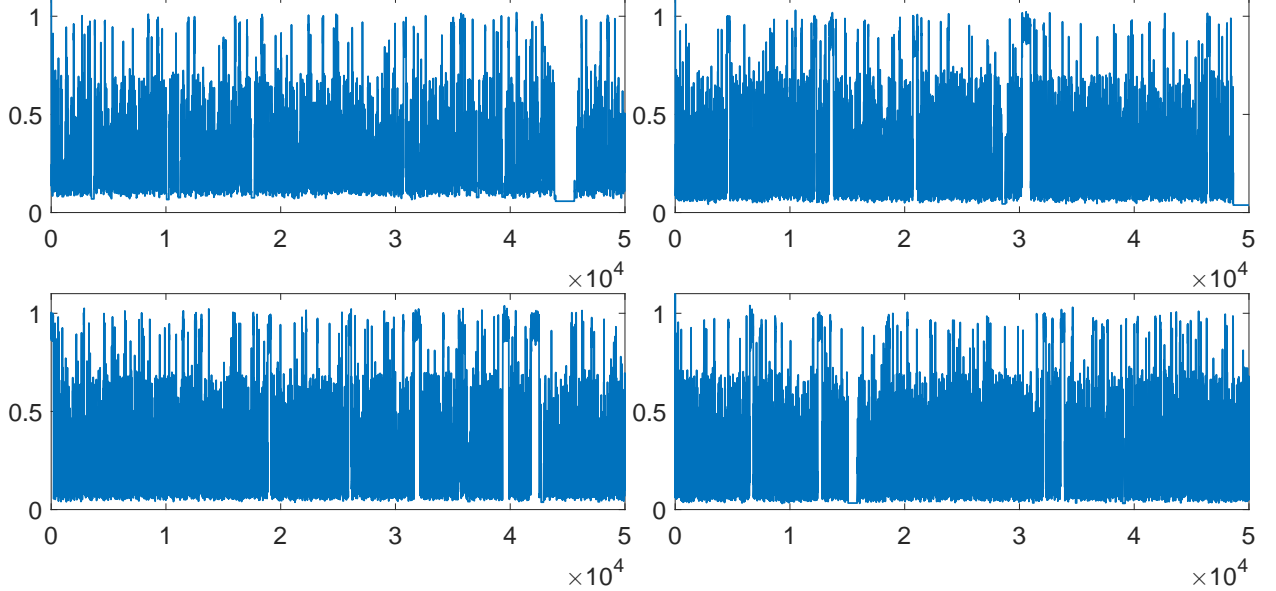


Figure 5: Traces for parameter  $\lambda$  for the **PM-HMC sampler**. From top left to bottom right:  $N = 16, N = 64, N = 128, N = 256$ .

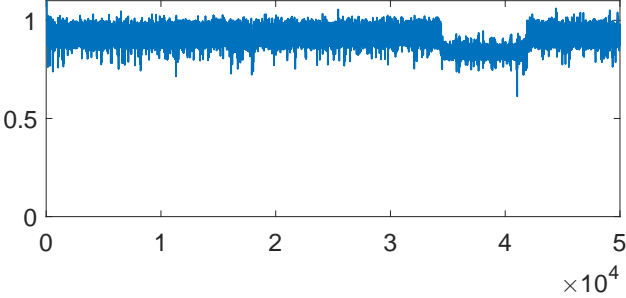


Figure 6: Traces for parameter  $\lambda$  for the **standard HMC sampler**, using a non-centered parameterisation. (Note that the sampler completely misses one mode of the posterior.)

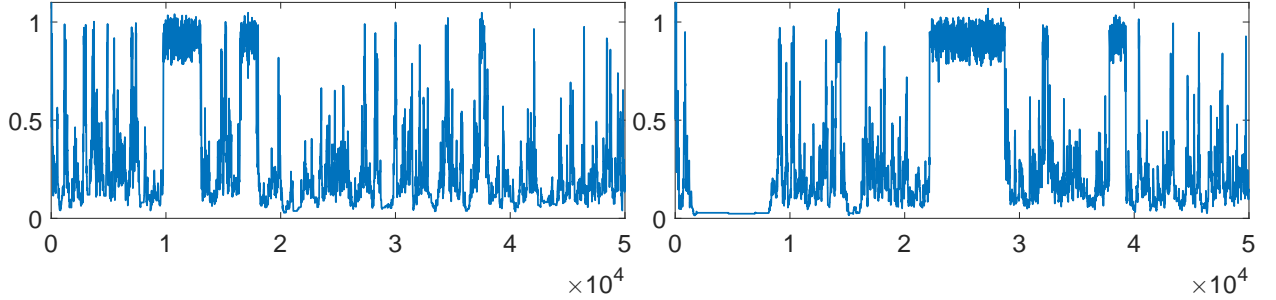


Figure 7: Traces for parameter  $\lambda$  for the **pseudo-marginal MH sampler** with  $N$  particles. Left,  $N = 512$ . Right,  $N = 1024$ .

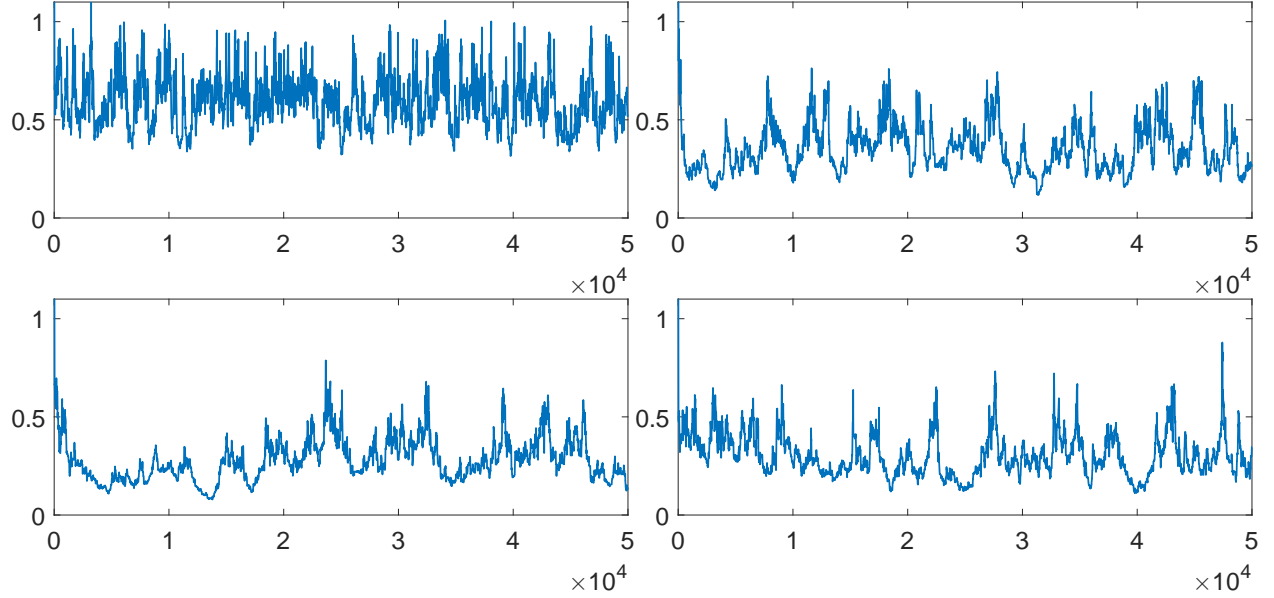


Figure 8: Traces for parameter  $\lambda$  for the **Gibbs sampler** using conditional importance sampling kernels with  $N$  particles to update the latent variables. From top left to bottom right:  $N = 16$ ,  $N = 64$ ,  $N = 128$ ,  $N = 256$ .

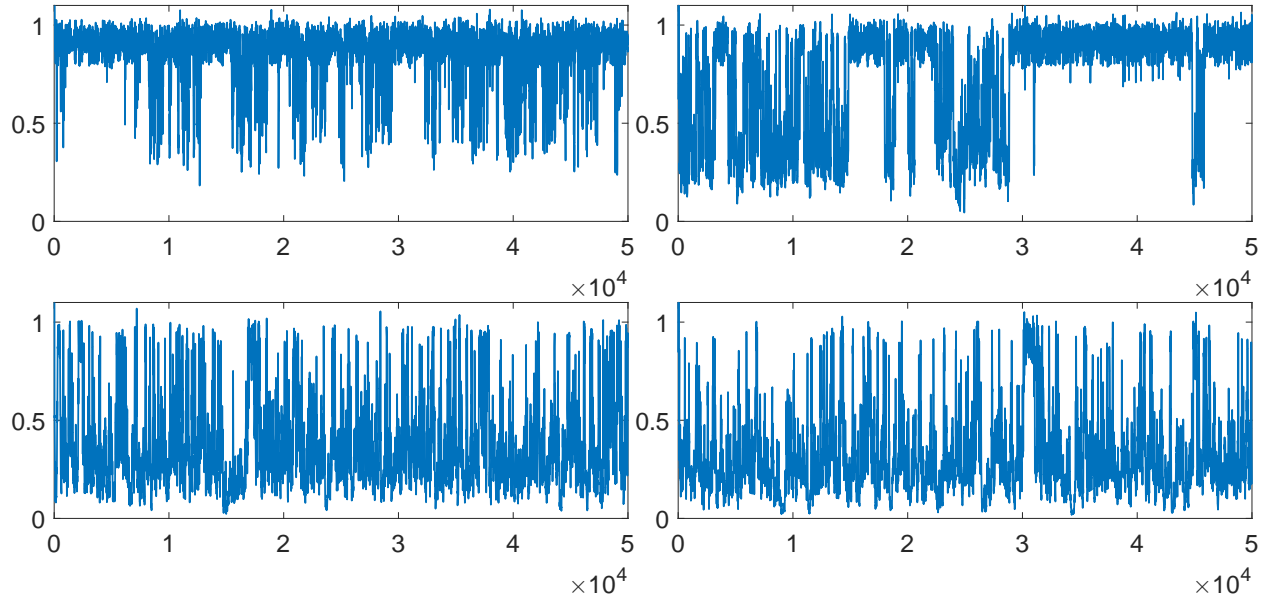


Figure 9: Traces for parameter  $\lambda$  for the **pseudo-marginal slice sampler**. From top left to bottom right:  $N = 16$ ,  $N = 64$ ,  $N = 128$ ,  $N = 256$ .

## D.2 Generalized linear mixed model

In this section we give some additional details and results for the generalized linear mixed model considered in Section 4.2 of the main manuscript.

The parameter values used for the data generation were:

$$\beta = \begin{pmatrix} -1.1671 & 2.4665 & -0.1918 & -1.0080 & 0.6212 & 0.6524 & 1.5410 & 0.2653 \end{pmatrix}^T,$$

$\mu_1 = 0$ ,  $\mu_2 = 3$ ,  $\lambda_1 = 10$ ,  $\lambda_2 = 3$ , and  $w_1 = 0.8$ .

All methods were initialized at the same point in  $\theta$ -space, as follows:  $\beta^{\text{init}}$  was sampled from  $\mathcal{N}(0, I_p)$ , resulting in:

$$\beta^{\text{init}} = \begin{pmatrix} 0.5838 & 0.3805 & -1.5062 & -0.0442 & 0.4717 & -0.1435 & 0.6371 & -0.0522 \end{pmatrix}^T,$$

whereas the remaining parameters were initialized deterministically as  $\mu_1^{\text{init}} = 0$ ,  $\mu_2^{\text{init}} = 0$ ,  $\lambda_1^{\text{init}} = 1$ ,  $\lambda_2^{\text{init}} = 0.1$ , and  $w_1^{\text{init}} = 0.5$ .

We used a  $\mathcal{N}(0, 100)$  prior for each component of  $\theta$ . However, for the particle Gibbs sampler we used a different parameterisation and (uninformative) conjugate priors when possible to ease the implementation. Varying the prior did not have any noticeable effect on the (poor) mixing of the Gibbs sampler.

For PM-HMC and the pseudo-marginal slice sampler we used a simple (indeed, naive) choice of importance distribution for the latent variables:  $q(x_i) = \mathcal{N}(x_i \mid 0, 3^2)$  since this was easily represented in terms of Gaussian auxiliary variables (which is a requirement for both methods). A possibly better choice, which however we have not tried in practice, is to use a Gaussian or  $t$ -distributed approximation to the posterior distribution of the latent variables. For the particle Gibbs sampler, which does not require the proposal to be represented in terms of Gaussian auxiliary variables, we instead used the (slightly better) proposal consisting of sampling from the prior for  $X_i$ .

The pseudo-marginal slice sampler made use of elliptical slice sampling for updating the auxiliary variables, as recommended by [18]. The components of  $\theta$  were updated one-at-a-time using random walk Metropolis-Hastings kernels. We also updating  $\theta$  jointly, but this resulted in very poor acceptance rates. The random-walk proposals were tuned to obtain acceptance rates of around 0.2–0.3.

The particle Gibbs sampler used conditional importance sampling kernels for the latent variables  $X_{1:T}$ , and for the parameters random walk Metropolis-Hastings kernels were used when no conjugate priors were available.

Figures 10–12 show trace plots for the four parameters  $\mu_1$ ,  $\mu_2$ ,  $1/\lambda_1$  and  $1/\lambda_2$  of the Gaussian mixture model used to model the distribution of the random effects. The three plots correspond to the pseudo-marginal HMC sampler, the pseudo-marginal slice sampler, and the Gibbs sampler with conditional importance sampling kernels, respectively. In Figure 13 we show estimated autocorrelations for the 13 parameters of the model for the three samplers.

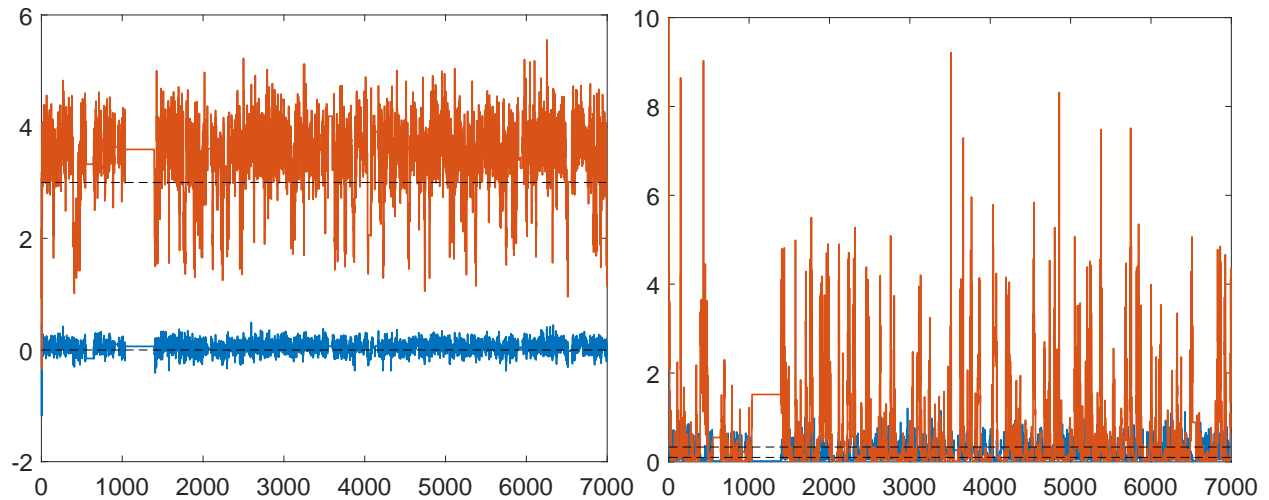


Figure 10: Traces for parameters  $\mu_1$  and  $\mu_2$  (left) and  $1/\lambda_1$  and  $1/\lambda_2$  (right) for the **pseudo-marginal HMC sampler** with  $N = 128$ .

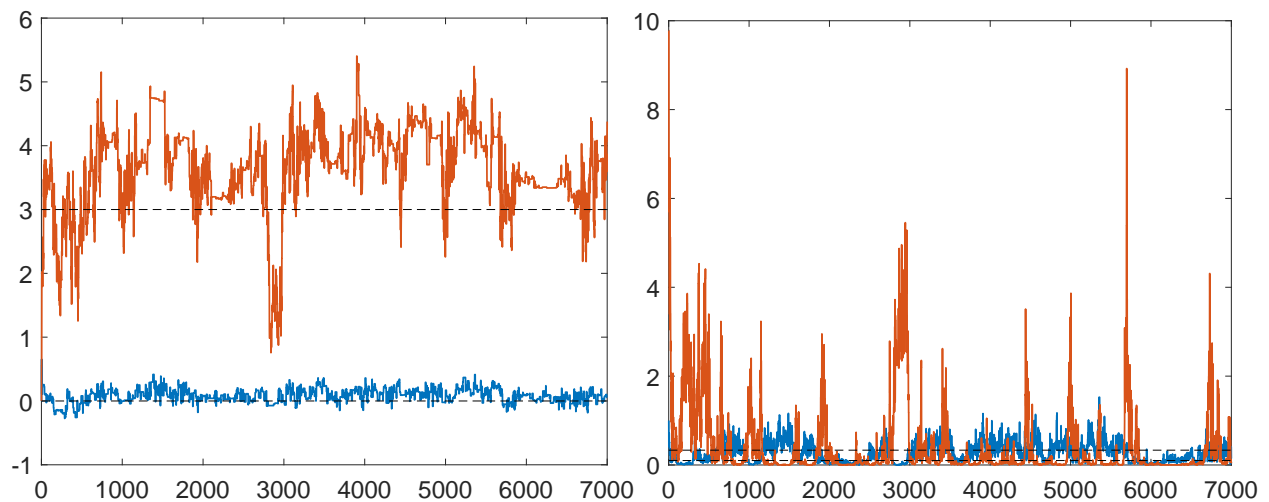


Figure 11: Traces for parameters  $\mu_1$  and  $\mu_2$  (left) and  $1/\lambda_1$  and  $1/\lambda_2$  (right) for the **pseudo-marginal slice sampler** with  $N = 128$ .

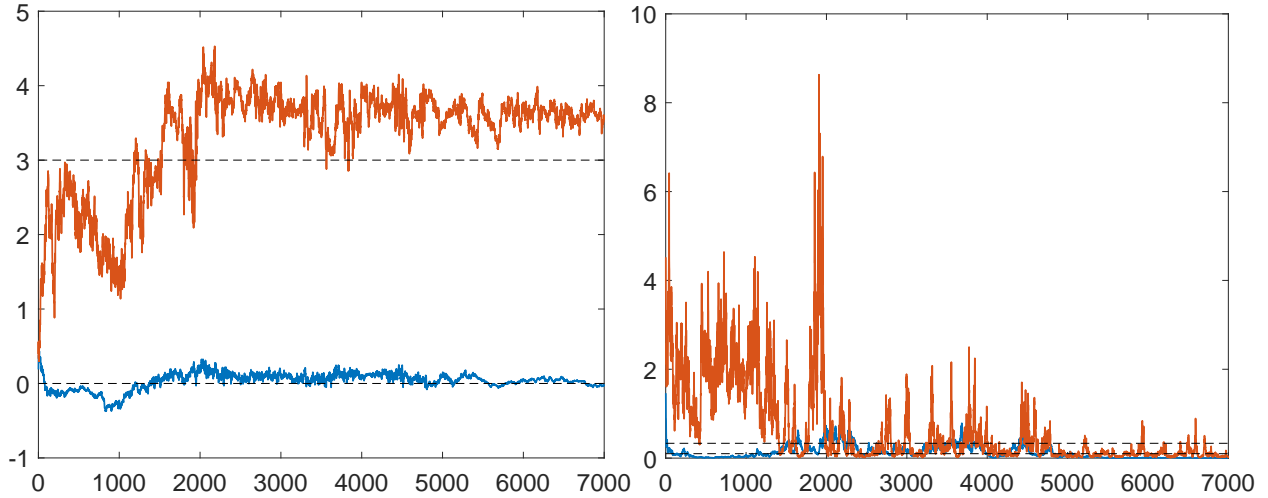


Figure 12: Traces for parameters  $\mu_1$  and  $\mu_2$  (left) and  $1/\lambda_1$  and  $1/\lambda_2$  (right) for the **Gibbs sampler** using conditional importance sampling kernels with  $N = 128$  particles to update the latent variables.

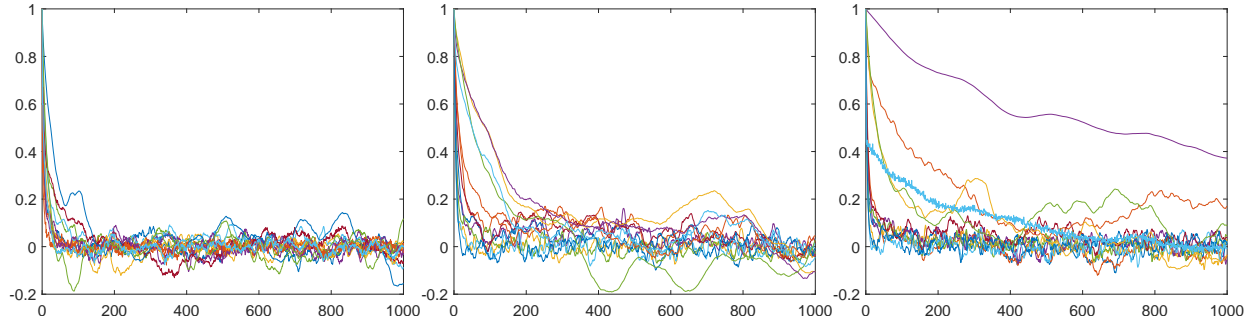


Figure 13: Estimated autocorrelations for the 13 parameters of the model for the **pseudo-marginal HMC sampler** with  $N = 128$  (left), **pseudo-marginal slice sampler** with  $N = 128$  (mid), and **Gibbs sampler** using conditional importance sampling kernels with  $N = 128$  particles to update the latent variables (right).